RIETI Discussion Paper Series 24-E-028

The Rise and Fall of Cities under Declining Population and Diminishing Distance Frictions: The case of Japan

MORI, Tomoya
RIETI

MURAKAMI, Daisuke
Institute of Statistical Mathematics

The Research Institute of Economy, Trade and Industry
https://www.rieti.go.jp/en/

RIETI Discussion Paper Series 24-E-028
February 2024

The Rise and Fall of Cities under Declining Population and Diminishing Distance Frictions: The case of Japan[1]

Tomoya Mori
Kyoto University and Research Institute of Economy, Trade and Industry

Daisuke Murakami
Institute of Statistical Mathematics

Abstract

Many countries are expected to face rapidly declining and aging populations. Meanwhile, urbanization continues worldwide, preserving the power law for city size distribution at the country level. We have developed a spatial statistical model based on the theory of economic agglomeration to predict the future geographic distribution of the population at the 1 km grid level. The model considers growth factors for cities and grids, while maintaining the power law for city size distribution at the country level. Japan is an ideal case study of a shrinking economy. It highlights the challenges that the rest of Asia and the world are likely to face. Cities in aging regions will decline more rapidly, shifting the center of gravity of the country's population distribution. Smaller cities are more vulnerable to population decline, but with declining transportation and communication costs, even large cities are not immune to elimination. The future urban economy will revolve around fewer and more distant larger cities.

Keywords: City growth, Aging, Distance friction, Power law, Sustainability
JEL classification: R12, R58, R41, R31, C15, C31

[1]This study is conducted as a part of the Project "Development of Quantitative Framework for Regional Economy Based on the Theory of Economic Agglomeration" undertaken at the Research Institute of Economy, Trade and Industry (RIETI). The authors would like to thank participants of the RIETI DP Seminar, where the draft of this paper was presented, for their helpful comments.
The authors are also grateful for helpful comments and suggestions by Keisuke Kondo (RIETI and Kobe University).

1 Introduction

Many developed countries around the world are expected to face aging and declining populations. This trend is particularly pronounced in Asian countries, where immigration is not a major contributor to population growth (Fig. 1A). Meanwhile, urbanization continues worldwide (United Nations, 2018, Fig. 1B for Asian examples). In a country where the population begins to decline while urbanization progresses, the number of sustainable cities necessarily decreases. In this paper, we propose a simple statistical model to predict the rise and fall of individual cities in a shrinking and aging economy. Japan is an ideal case study of such an economy. It highlights the challenges that the rest of Asia and the world are likely to face.

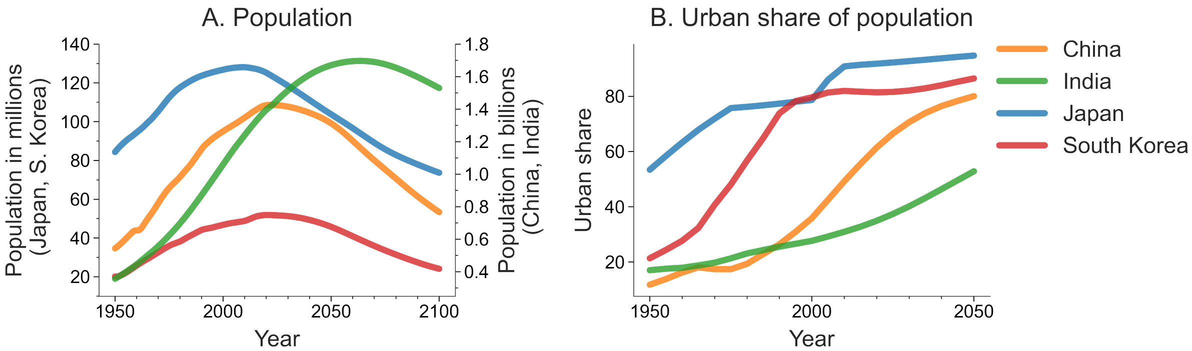

Figure 1. Forecasts of population and urban share of population in Asia

Notes: Data underlying the graphs in Panels A and B are obtained from United Nations (2022, 2018), respectively.

We consider a city as a population agglomeration whose geographic extent evolves over time in response to the changes in the conditions in its nearby area as well as those at the county level. Looking at the regional economy through the lens of cities, a clear structure emerges. It is well known that the distribution of city sizes within a country generally follows a power law (e.g., Gabaix and Ioannides, 2004), a phenomenon not seen in other regional aggregates such as administrative regions (Fig. 2). Although often abstracted in the literature (e.g., Behrens et al., 2014; Duranton and Puga, 2014, §5.7), the relationship between population and geographic arrangement of cities is not random, but is generally characterized by a recursively nested regional structure, with each nested region consisting of a group of small cities surrounding a large one whose city size distribution follows a similar power law (Mori et al., 2020). The fact that national economic geography manifests such a spatial fractal structure with a power law for city size has already been given a theoretical explanation by modern central place theory (Hsu, 2012; Mori et al., 2023a).

In this paper, we propose a framework for predicting the evolution of the geographic population distribution in the national geography of Japan at the 1 km grid level. Our forecasting model is obtained by ensembling statistical models that account for both

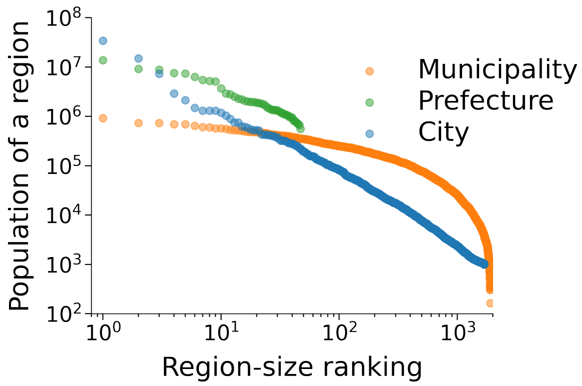

Figure 2. The size distributions of prefectures, municipalities and cities in Japan

Notes: Each city in Japan in 2020 was identified as the set of 1km grid cells that (i) have a population density of at least 1,000 per square kilometer, (ii) are geographically contiguous, and (iii) have a total population of at least 1,000. Population count data in 30″×45″ grids were obtained from the Grid Square Statistics of the 2020 Population Census of Japan. The graphs include 46 prefectures, 1,907 municipalities, and 1,965 cities in the Japanese archipelago that are connected by road to the four major islands of Japan, Hokkaido, Honshu, Shikoku, and Kyushu in 2020. The horizontal axis shows the ranking of regions by their population size, and the vertical axis shows their population size.

grid- and city-level growth factors, and a model that imposes a city growth process consistent with a power law for the national city size distribution. We update the set of cities at each point in time by identifying each city as a population agglomeration over a contiguous set of 1 km grid cells, whose intertemporal evolution we track over time.

We begin by showing that the evolution of Japan's cities over the past half century is highly consistent with the theory of economic agglomeration (Akamatsu et al., 2023). During this period, Japan experienced a substantial reduction in transportation and communication costs. Specifically, Japan's nationwide high-speed rail and highway networks were developed from scratch and gradually expanded into nationwide networks. Meanwhile, the Internet was introduced and became ubiquitous throughout the country, reducing communication costs.

The theory of economic agglomeration (Akamatsu et al., 2023; Mori et al., 2023b) predicts that reduced transportation costs will facilitate the concentration of population into larger and fewer cities, thus skewing the distribution of city sizes towards larger cities. Within a city, on the other hand, they induce a dispersion of population in the form of a flattening of cities. For a given population size of a city, the residential distribution will spread over a larger area, decreasing both the maximum and the average population densities (Fig. 5). In addition to the persistent power law for city size distribution at the country level, this is exactly what has happened in Japan over the past half century (see Figs. 6 and 7). With the rapid advance of automated logistics systems and virtual communication technologies, a further and unprecedented reduction in distance friction is one of the obvious future trends that we can expect. The theory therefore suggests that the trend we have seen over the past half century will continue in the future.

Of course, what we observed in the evolution of cities is a consequence of a number of factors, not just the reduction of transportation and communication costs. Nevertheless, the theory of economic agglomeration seems to be a strong predictor of the evolution of cities, as it can simultaneously explain the concentration toward larger cities at the country level and the flattening of individual cities, while maintaining the power law for the distribution of city sizes over the past half century.

Thus, we train our statistical model on the evolution of Japanese cities over the past half-century and take the trend of declining transportation costs over this period as the baseline for the future. Otherwise, our baseline projection extrapolates the spatial distribution of population into the future under the official projection of Japan's total population obtained from National Institute of Population and Social Security Research (NIPSSR) (2023b) (Fig. 8A) and the observed trend of urbanization (Fig. 8B).

We confirm that the predicted rise and fall of cities is consistent with the theoretical implications (Akamatsu et al., 2023; Mori et al., 2023b). Namely, we continue to observe concentration toward larger and fewer cities, whereas smaller cities and cities in less advantageous locations are shuffled out and disappear. Cities will generally flatten out over a larger area, while reducing their maximum population density. However, there is a large regional variation in the rise and fall of cities, which appear to depend on their relative location and the aging of their residents.

Other than Tokyo, the only city projected to see a significant increase in population share is Fukuoka, which is currently the fourth largest city. Fukuoka has the advantage of being outside the influence of Tokyo's urban agglomeration, unlike the second and third largest cities, Osaka and Nagoya, which lie between Tokyo and Fukuoka. Fukuoka's population share will increase by 61% between 2020 and 2120, while those of Osaka and Nagoya will remain unchanged. Cities in aging eastern regions will decline more rapidly, causing the center of gravity of population distribution to shift toward the western part of the country.

We also attempt future projections of the spatial distribution of the population under alternative rates of reduction in distance friction over time. These exercises allow us to face a rapidly shrinking economy and stay ahead of the curve in developing sustainable regional policies by identifying sustainable cities and the underlying factors for sustainability.

The rest of the paper is organized as follows. We begin in Section 2 with the strong correspondence between the observed evolution of cities and the theory of economic agglomeration on which our statistical forecasting model is based. In Section 3, we describe the basic data and explain how we track the evolution of individual cities over time. In Section 4, we introduce our statistical forecasting model and demonstrate the importance of city-level aggregation in predicting the future geographic distribution of the population. In Section 5, we present our baseline projections of city growth and shrinkage through 2200, and discuss the relationship between aging and city growth. In Section 6, we explore alternative scenarios regarding the rate of reduction of distance friction, as reflected in the rate of change of the power law coefficient. In Section 7, we discuss the implications of our predictions for place-based policy, housing policy, urban planning, and disaster risk management in cities.

2 Facts and theory about the evolution of cities in Japan

In this section, we show how useful the theory of economic agglomeration is in explaining the geographic distribution of the population and its responses to changes in key parameters. Our main data for estimating the model are the population counts in 30″×45″ grids (approximately 1 km by 1 km) obtained from the Grid Square Statistics of the Population Census of Japan by Ministry of Internal Affairs and Communications of Japan (MIAC hereafter) for every five years from 1970 to 2020. This last half-century of Japan is an ideal period for our purpose.

Throughout the paper, each city is identified as a *Urban Agglomeration* (*UA*) defined by a spatially contiguous set of grids with a population density of at least 1,000 per 1 km^2 and a total population of at least 10,000. The red areas in Figure 3 indicate the 431 UAs in 2020 identified using this definition. These UAs account for 80% of Japan's population while occupying 6% of the total land area. The urban share of population has kept increasing, and the geographical organization of the population is essentially dominated by cities.

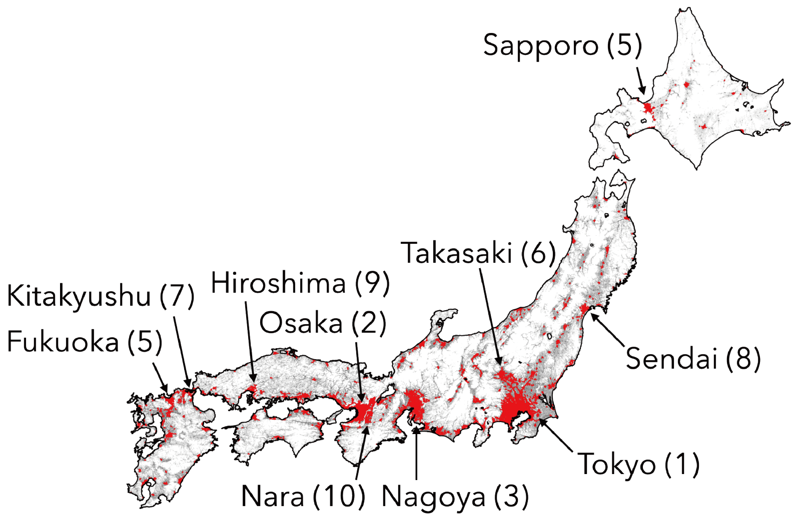

Figure 3. Cities in Japan in 2020

Notes: Each disjoint red area is an urban agglomeration. The 10 largest cities in 2020 are listed, with the numbers in the parentheses indicating their ranking by population size. The figure is linked to a web map showing the geographic distribution of the population in Japan which can be scrolled and zoomed in. Yellow and warmer colors indicate the grid cells with a population density at least 1,000.

Japan's population has been growing since the beginning of time, except for short-term declines due to wars and natural disasters, and reached 104 million in 1970 at the beginning of our study period. However, after reaching its peak of 128 million in 2010, it began to decline and reached 127 million in 2020. Thus, the 1970-2020 period includes this turning point.

This is also the period in which Japan's high-speed railways and highways were developed almost from scratch into full-fledged nationwide networks. Construction of Japan's high-speed railways and highways began in time for the 1964 Tokyo Olympics. The total length of high-speed railways (highways) increased from 515 km (216 km) in 1964 to 3,067 km (13,189 km) in 2020, significantly reducing transportation costs in Japan (Fig. 4). Meanwhile, the Internet was introduced in the 1990s and became ubiquitous throughout the country in the 2000s and beyond, also significantly reducing communication costs.

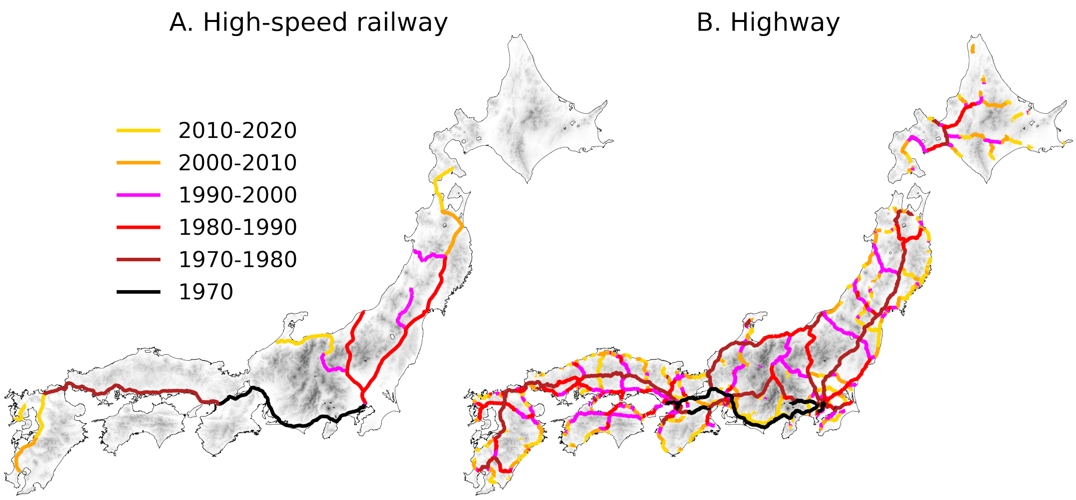

Figure 4. The development of high-speed transportation networks in Japan between 1970 and 2020

Notes: The shapefiles of the transport networks are obtained from the National Land Numerical Information Download Service (NLNI) by the Ministry of Land, Infrastructure, Transport and Tourism (MLIT) of Japan (https://nlftp.mlit.go.jp/).

Akamatsu et al. (2023) have shown that the most general class of microeconomic models of economic agglomeration in the literature exhibit the response to the reductions in transportation costs shown in Figure 5.[1] On the one hand, at the country level, competition is becoming more global, and the market areas of firms in neighboring cities are beginning to overlap. As a result, the economic hinterlands of these cities start to interfere with each other, and some cities are squeezed out. The surviving cities will be farther apart and will grow in size by attracting population from the declining

[1]Here, we exclude the large literature on the systems-of-cities models (see, e.g., Duranton and Puga, 2014), since they cannot address the geographic distribution of cities and has little to say about the location of cities as they abstract from inter-city space.

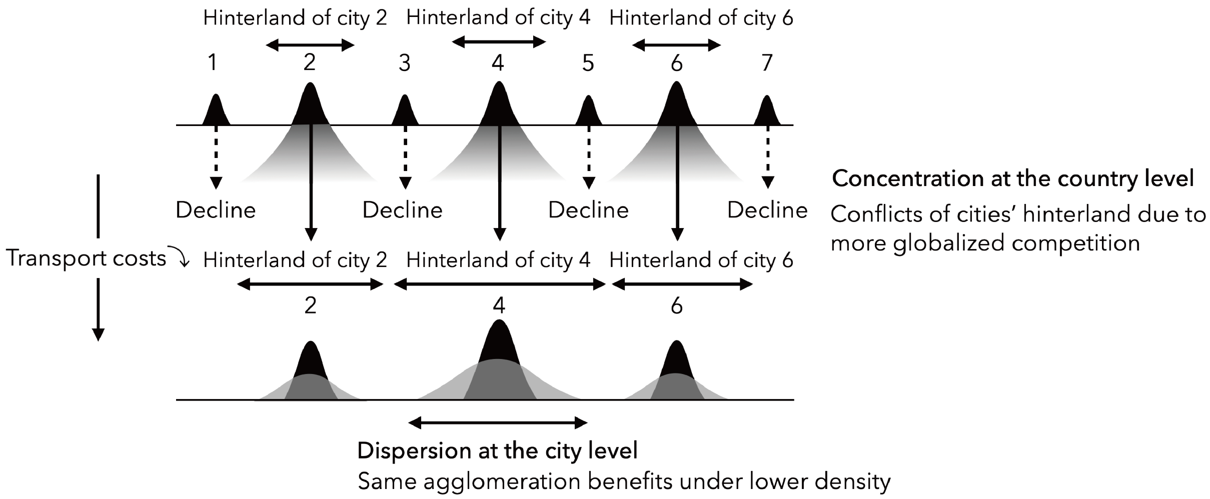

Figure 5. Cities' response to the reduced transport costs

cities. On the other hand, at the city scale, both firms and workers have less incentive to concentrate near the city center and disperse in search of cheaper space. As a result, cities become flatter and more sprawling.

Figures 6 and 7 summarize what actually happened to cities in Japan during the period 1970-2020. At the country level, the number of cities was 504 in 1970. It peaked at 511 in 1975, at the end of Japan's high-growth era, and continued to decline to 431 in 2020. Meanwhile, the distribution of city size has become clearly skewed toward larger cities (Fig. 6), with larger cities becoming larger and smaller cities becoming smaller.

Within a city, the average and maximum population densities continued to decrease, and the area occupied by a city continued to increase. Specifically, the average and maximum population densities decreased by an average of 24% and 35%, respectively, and the area occupied by a city increased by an average of 86% (Fig. 7), while the total population of Japan increased by 22%. Thus, cities have clearly flattened out.

As discussed in the Introduction, we still expect a substantial reduction in distance frictions in the coming century with rapidly advancing automated logistics systems and virtual communication technologies. Thus, we expect a qualitatively similar evolution of cities in the future, where there will be a concentration towards larger and fewer cities, while each surviving city will flatten out. In addition, we have a declining population that is shifting the distribution of city sizes downward, so that more cities will be eliminated in the next half century than in the last half century. An important validation of our forecasting model is the qualitative consistency of its future projections with theory.

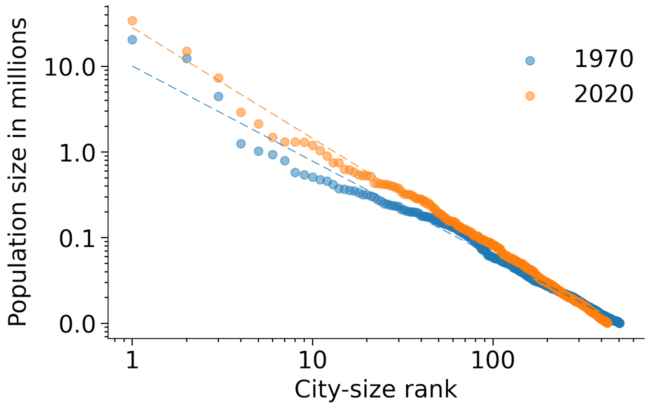

Figure 6. Concentration at the country level

Notes: City size distributions of Japan in 1970 and 2020. Cities are identified as explained in Fig. 2. The dashed lines are the fitted lines obtained from the log-linear regression of population size on the rankings of cities in terms of population size.

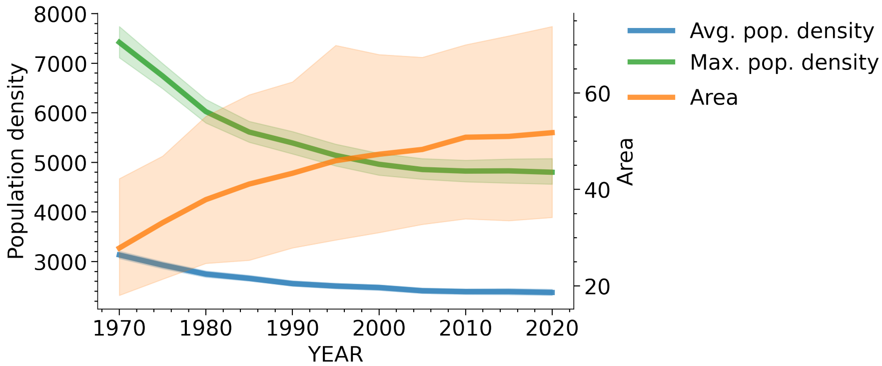

Figure 7. Dispersion at the city level

Notes: The blue and green lines show the means of average and maximum population densities of a city and the orange line the mean total area of a city for each year indicated along the horizontal axis, while the shaded area indicates the range covering 90% of the values for individual cities.

3 The basic setup and data preparation

Our goal is to predict the sustainability of individual cities in a future of rapid population decline. Even in Japan, a country at the forefront of population decline, population decline has only become apparent since the 2010 census, which is a relatively recent phenomenon. Therefore, it is not advisable to use long time-series data going back in time to predict the rise and fall of cities over the next 50 to 100 years, as it is likely to underestimate population decline.

In the case of Japan, geographic population distribution data for the entire country prior to 1970 are only available at the municipal level and thus have a much different resolution than the post-1970 grid data. Although the time series data used to train the model is short (11 time points), we believe that overall it provides more appropriate learning data than adding earlier data with different trends and resolutions. Our main data for training the model are the population counts in the 1-km grid cells obtained

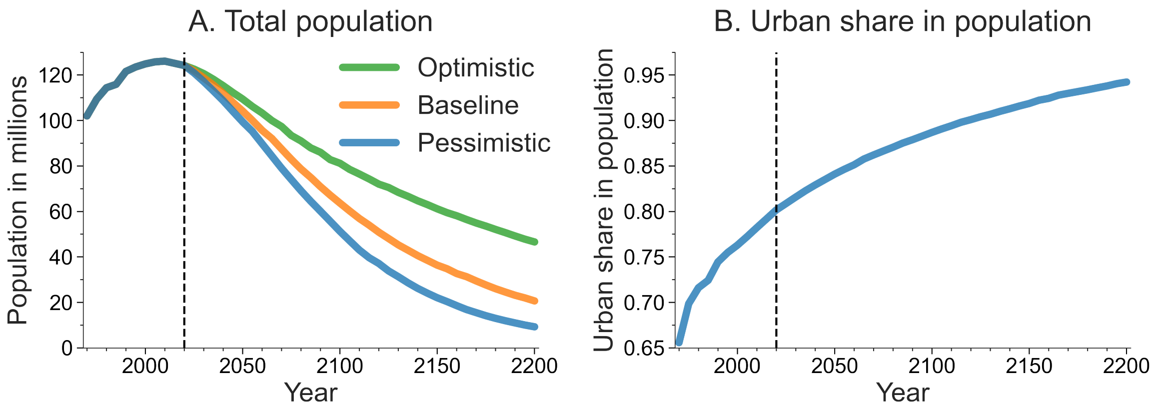

Figure 8. Forecasts of total population and urbanization in Japan

Notes: (A) Japan's population for 1970–2020 is the observed value. Population projections for 2021 to 2120 were obtained from National Institute of Population and Social Security Research (2023a). The baseline projection assumes the fertility rate, 1.36, and mortality rate in 2020 will persist in the future, while the pessimistic (optimistic) projections assumes lower (higher) fertility rate, 1.13 (1.64), and higher (lower) mortality rate will persist in the future. We extrapolated the projections to 2200 using spline-based smoothing. (B) Urban share of total population. Observations in 1970–2020 are extrapolated to 2200 by assuming that the urban share increases log-linearly over time.

from the Grid Square Statistics of the Population Census of Japan for every five years from 1970 to 2020.

The period of the last 50 to 20 years, when the declining population trend became more pronounced not only in Japan but also in other countries, coincides with the development of high-speed transportation networks and the spread of the Internet. Thus, these data from recent decades are suitable for incorporating the effect of reducing distance frictions, which is expected to continue in the future due to advances in automated driving and logistics, as well as video, voice, and communication technology.

To project the geographic distribution of the population in Japan in the future, we take as given the official projection of the total population of Japan provided by NISSR (2023a) for the years 2025 to 2120. There are three versions, each of which assumes that fixed fertility and mortality rates will continue into the future. These rates are set to the 2020 values for the baseline case. We have extrapolated the projections to 2200 by applying a spline-based smoothing (Fig. 8A). We also assume that the urbanization trend of the last 50 years will continue into the future. Since the urban share of the population has a simple monotonic trend in the past, we extrapolate it by assuming a log-linear function of time (Fig. 8B).

Let $t \in \{1,\ldots,36\}$ represent the time index of the t-th year in the period 1970–2200 by 5-year intervals (i.e., $t = \frac{year-1965}{5}$). The set of cities is updated every t, new cities may form, several cities may merge, and a city may split, disappear, and reappear. We track each city over time based on the overlap of its spatial area at different time points, assigning it a unique identifier throughout the study period (see Appendix A for details).

4 A forecasting model of city growth and decline

Our forecasting model has three levels: country, city, and grid levels. The country-level model accounts for the growth process of cities, consistent with the power law for city size distribution. The city- and grid-level models are time-series models for each city and grid, respectively, accounting for city- and grid-specific growth factors. At the grid level, we also account for the spatial correlation of growth in the area surrounding each grid.

The spatial coverage of each city changes, which is captured by reidentifying the set of cities at each point in time. Thus, the set of cities is endogenous, where there are births, splits, and disappearances of cities. This section describes the details of each model, how we ensemble them, and how we proceed to forecast the future set of cities.

4.1 The country-level model

It is assumed that cities tend to follow the power law for their (population) size distribution at the country level. The city size distribution may temporarily deviate from the power law due to idiosyncratic factors at the city and grid level, or due to bifurcations of an equilibrium at the country level (e.g., births and deaths of cities).

Let $\mathbf{U}_t$ be the set of cities in time t, $P_{u,t}$ represent the size of city $u \in \mathbf{U}_t$, and $R_{u,t}$ its ranking in terms of size in time t. The city sizes distribution is assumed to roughly follow the power law, which is empirically expressed as

$$\log P_{u,t} = A_t + B_t \log(R_{u,t} - 0.5) + \epsilon^{PL}_{u,t}, \quad \epsilon^{PL}_{u,t} \sim N(0, \sigma^2_{P,u}), \tag{1}$$

where "−0.5" is a bias correction (see Gabaix and Ibragimov, 2011), and $\sigma^2_{P,u}$ is a variance parameter. The parameters A_t and B_t represent the population scale and power coefficient, respectively.

Populations are concentrated in larger cities, as B_t becomes negatively larger as in the case of the last half century in Japan (Fig. 6). As we have discussed in Section 3, to project population concentration/dispersion in the future, these parameters are assumed to monotonically change over time, following the log-linear models,

$$A_t = a^A_0 + a^A_1 \log t + \epsilon^A_{u,t}, \quad \epsilon^A_{t,u} \sim N(0, \sigma^2_A), \tag{2}$$

$$B_t = a^B_0 + a^B_1 \log t + \epsilon^B_{u,t}, \quad \epsilon^B_{t,u} \sim N(0, \sigma^2_B), \tag{3}$$

where $a^A_0, a^A_1, a^B_0, a^B_1, \sigma^2_A$, and σ^2_B are the parameters to be estimated.

PL: Power-law model

To obtain the growth process of a city consistent with the power law for the city size distribution, the conditional expectation $E[P_{u,t+1}|P_{u,t}] = \hat{P}_{u,t+1}$ is obtained by differencing (1) with respect to t after substituting eqs. (2) and (3) as follows:

$$\hat{P}^{PL}_{u,t+1} \equiv P_{u,t} + \Delta P_{u,t} = P_{u,t} + \frac{a_1^A + a_1^B \log(R_{t,u} - 0.5)}{t} P_{u,t}. \tag{4}$$

This equation performs one-step-ahead prediction assuming faster (slower) population growth in higher ranked city if $a_1^B < 0 (> 0)$.[2]

4.2 City-level models

In the PL model, future city size rankings remain constant. In reality, however, there are deviations from the power law, and the size rankings of cities change. These deviations may result from location-specific factors or from the bifurcation of the equilibrium of a city system (e.g., Akamatsu et al., 2023) triggered by the change in parameter values.[3] For example, Osaka, the second largest city in Japan, has been in decline since 2000. Osaka is the only one among the top five that has experienced a population decline since 2000. After the introduction of the faster and more frequent Nozomi express train in 1992 on the bullet train line connecting Osaka and Tokyo, the economic distance between these two cities decreased significantly. According to the theory of economic agglomeration, Osaka became too close to Tokyo to maintain its current population size, and thus its growth process deviated from the power law of city size.

To complement the PL model, we introduce time-series models to capture city-specific growth factors. Relevant time-series models include the autoregressive integrated moving average (ARIMA) model (Box et al., 2015), the state-space model (SSM; see Durbin and Koopman, 2012), and recurrent neural networks (RNN; see Graves, 2013). The relevant observed time series data are typically too short for our forecasting model (only 11 time steps in our case) to apply SSM and RNN. Even for the ARIMA model, which is simpler than SSM and RNN, our preliminary analysis showed that the projected population often takes extremely large or small values given our long projection period of a century or more. Therefore, we use simpler time-series models.

Let ARIMA(p,d,q) represent an ARIMA model with an autoregressive process of

[2]Note that this growth process does not necessarily have a stationary state. However, since our one-step-ahead projection procedure (introduced in Section 4.4) always converges, it empirically proves to be a stationary process.

[3]The changes in the rankings of cities in terms of population size are often attributed to random factors in the literature on city systems models (e.g., Duranton and Puga, 2014, 2023), there are actual cases suggesting deterministic factors implied by the new economic geography models (e.g., Akamatsu et al., 2023) as discussed below.

order p, a moving average process of order q, and a difference of order d. We consider the four models below to explain the growth of city u.

ARI1: the ARIMA(1,1,0) model

$$\Delta P_{u,t+1} = \rho_u \Delta P_{u,t} + \epsilon_{u,t}^{ARI1}, \quad \epsilon_{u,t}^{ARI1} \sim N(0, \sigma_{u,ARI1}^2). \tag{5}$$

where $\Delta P_{u,t+1} \equiv P_{u,t+1} - P_{u,t}$. The auto-correlation coefficient ρ_u takes a positive value in the presence of positive temporal correlation while the opposite is true for negative correlation. We used a difference auto-regressive process because differentiation eliminates non-stationary trends such as depopulation in recent years. To estimate the difference in population growth pattern by city, parameters are estimated by city using a maximum likelihood method.

ARI2: the ARIMA(2,1,0) model

$$\Delta P_{u,t+1} = \rho_{1,u} \Delta P_{u,t} + \rho_{2,u} \Delta P_{u,t-1} + \epsilon_{u,t}^{ARI2}, \quad \epsilon_{u,t}^{ARI2} \sim N(0, \sigma_{u,ARI2}^2), \tag{6}$$

which models second order time series using parameters $\rho_{1,u}$ and $\rho_{2,u}$. Because of the limited time periods, we do not consider higher order dependence. In addition, since the moving average process only explains short-term dependence, we ignore it (e.g., the second-order moving average process only affects the second period ahead).

CS: Constant model

$$P_{u,t+1} = P_{t,u} + \epsilon_{u,t}^{CS}, \quad \epsilon_{u,t}^{CS} \sim N(0, \sigma_{u,CS}^2), \tag{7}$$

which assumes constant population in the future.

LL: Log-linear-in-time model (Smith et al., 2005)

$$P_{u,t+1} = a_{u,0}^{LL} + a_{u,1}^{LL} \log t + \epsilon_{u,t}^{LL}, \quad \epsilon_{u,t}^{LL} \sim N\left(0, \frac{\sigma_{u,LL}^2}{t^2}\right), \tag{8}$$

where $a_{u,0}^{LL}$ and $a_{u,1}^{LL}$ are regression coefficients. The model is estimated to minimize the least squares error weighted by t^2, with a greater weight in time t or just before. Also, according to Smith et al. (2005), the estimated intercept $\hat{a}_{u,0}^{LL}$ is shifted to equate the predicted value in 2020 with the observed value, so that the predictive function is shifted, so that the function passes through the actual population in 2020.

All the time-series models are estimated by city and assume Gaussian predictive distributions $N(\hat{P}_{u,t+1}^M, \hat{V}_{u,t+1}^M)$ where $M \in \{ARI1, ARI2, CS, LL\}$. As derived in Bromiley (2003), Gaussian (predictive) distributions can be synthesized by taking the product of their probability density functions (see also Cohen et al., 2020). The synthesized predictor of time-series (TS) models obeys a Gaussian distribution $N(\hat{P}^{TS}_{u,t+1}, \hat{V}^{TS}_{u,t+1})$ with predictive mean

$$\hat{P}^{TS}_{u,t+1} = \frac{\Sigma_M W^M_{u,t+1} \hat{P}^M_{u,t+1}}{\Sigma_M W^M_{u,t+1}}, \tag{9}$$

and the predictive variance $\hat{V}^{TS}_{u,t+1} = \frac{1}{\Sigma_M W^M_{u,t+1}}$ where $W^M_{u,t+1} = \frac{1}{\hat{V}^M_{u,t+1}}$. By assuming that $\hat{V}^M_{u,t+1} \propto \hat{V}^M_{u,2020}$, i.e., the relative accuracy of the M-th model is unchanged over years, it is imposed that $W^M_{u,t+1} \propto 1/Var(\hat{P}^M_{u,2020})$ where the variance is evaluated by projecting the UA population in 2020 by fitting each model to city populations up to 2015.

Unlike model selection, which is commonly used in ARIMA-based modeling, this model aggregation/averaging reduces the predictive variance and improves the stability of the projection (Polikar, 2012). Since this property is helpful in our case with limited time periods, we rely on model averaging.

Finally, the model for predicting the population size of each city u is obtained by ensembling the PL and TS models, eqs. (4) and (9), as follows.

$$\hat{P}_{u,t+1} = \frac{W^{TS}_u \hat{P}^{TS}_{u,t+1} + W^{PL}_u \hat{P}^{PL}_{u,t+1}}{W^{TS}_u + W^{PL}_u}. \tag{10}$$

4.3 Grid-level models

Let $\mathbf{G}$ represent the set of grids in Japan. Based on the discussion in Section 4.2, we again rely on simple time-series models, which are suitable in our setting, to project population $p_{i,t}$ for $t \in \{12, \ldots 36\}$ in grid $i \in \mathbf{G}$. The following models are considered to predict the population growth pattern in each grid:

- ARI1 model, i.e., ARIMA(1,1,0) (see eq. (5))
- ARI2 model, i.e., ARIMA(2,1,0) (see eq. (6))
- CS model (see eq. (7))
- LL model (see eq. (8))

To capture the population growth pattern in the neighboring areas, the same models are applied to the population $q_{i,t}$ in the 9 nearest neighbor grids (9NN):[4]

- $\mathrm{ARI1_N}$ model: The ARI1 model for $q_{i,t}$
- $\mathrm{ARI2_N}$ model: The ARI2 model for $q_{i,t}$

[4]The 9NN of a grid i includes the edge- and point-adjacent neighbors of grid i, including grid i itself. While each 9NN of grid i has at most 9 grid cells, it may have fewer grid cells if, for example, grid i is located at the coast.

- $\mathrm{CS_N}$ model: The CS model for $q_{i,t}$
- $\mathrm{LL_N}$ model: The LL model for $q_{i,t}$

The above four models, which are estimated by using the 9NN population data up to 2020, are applied to project future population of the 9NNs. The projected population $\hat{q}_{i,t}$ is then used to predict the gridded population $p_{i,t}$ by substituting $\hat{q}_{i,t}$ into

$$p_{i,t} = b_i \hat{q}_{i,t} + \epsilon_{i,t}, \quad \epsilon_{i,t} \sim N(0, s^2). \tag{11}$$

The parameter b_i is estimated a priori by regressing the gridded population $p_{i,t}$ in 2020 on the 9NN population $q_{i,t}$.

Since the eight models assume Gaussian errors, they can be synthesized by taking the product of their Gaussian predictive distributions, as done in the city-level projection. The synthesized predictive distribution obeys $N(\hat{p}_{i,t}, \hat{v}_{i,t})$ with predictive mean

$$\hat{p}_{i,t} = \frac{\Sigma_m w_{i,t}^m \hat{p}_{i,t}^m}{\Sigma_m w_{i,t}^m} \tag{12}$$

and predictive variance $\hat{v}_{i,t} = \Sigma_m \frac{1}{\hat{v}_{i,t}^m}$ where m denotes the four grid-level time-series models, $\{ARI1, ARI2, CS, LL\}$, and four 9NN-level time-series models, $\{ARI1_N, ARI2_N, CS_N, LL_N\}$. $\hat{v}_{i,t}^m$ is the predictive variance of model m in 2020 evaluated by another population projection using data between 1970 and 2015. This model averaging step implicitly determines the strength of the grid-specific growth pattern and the growth pattern that is common across the 9NN based on the predictive accuracy.

4.4 Projection procedure

We use the gridded population data for the period 1970–2020 (every 5 years) from the Population Census of Japan to estimate the baseline model (see Appendix B.1 for details). We then start predicting for $t = 12$ from $t = 11$, which is the last time point (year 2020) in the observed data. We are at **Step 1** in the flowchart in Figure 9, where $\hat{\boldsymbol{P}}_t \equiv \{\hat{P}_{u,t} : u \in \mathbf{U}_t\}$ and $\hat{p}_t \equiv \{\hat{p}_{i,t} : i \in \mathbf{G}\}$. For $t = 11$ (year 2020), $\hat{P}_{u,11} \equiv P_{u,11}$ and $\hat{p}_{i,11} \equiv p_{i,11}$ are the observed values.

In **Step 2**, we perform a one-step-ahead prediction under each of the city-level and grid-level models introduced in Sections 4.2 and 4.3. In **Step 3**, we ensemble them according to eqs. (10) and (12). In **Step 4** we simulate the stationary geographic population distribution over the grids, consistent with the country and city level growth factors.

We first rescale the grid population to be consistent with the city population and the city population to be consistent with the country population. For a given prediction

$\{\hat{\boldsymbol{P}}_{t+1}, \hat{\boldsymbol{p}}_{t+1}\}$ of **Step 3** under $\mathbf{U}_t$, we rescale the grid population $\hat{p}_{i,t+1}$ in the grid $i \in \mathbf{U}_{u,t}$ to be consistent with the city population $\hat{P}_{u,t+1}$ (see Appendix **??**), and rescale the city population $\{\hat{\boldsymbol{P}}_{t+1}\}$ to be consistent with the country population in $t+1$ (see Appendix B.2).

Next, we re-identify cities based on the city definition (see Appendix A) to obtain the new city set $\mathbf{U}_{t+1}$. We then plug the rescaled $\{\hat{\boldsymbol{P}}_{t+1}, \hat{\boldsymbol{P}}_{t+1}\}$ into **Step2** to perform a one-step-ahead projection to obtain the updated set of city and grid populations $\{\hat{\boldsymbol{P}}'_{t+1}, \hat{\boldsymbol{P}}'_{t+1}\}$. as well as the updated city set $\mathbf{U}'_{t+1}$. This process is repeated until the original and updated city sets coincide, i.e., $\mathbf{U}_{t+1} = \mathbf{U}'_{t+1}$ (see B.2 and B.3 for details).

In our application to Japanese cities, this iteration converges to a non-degenerate geographic distribution of the population.

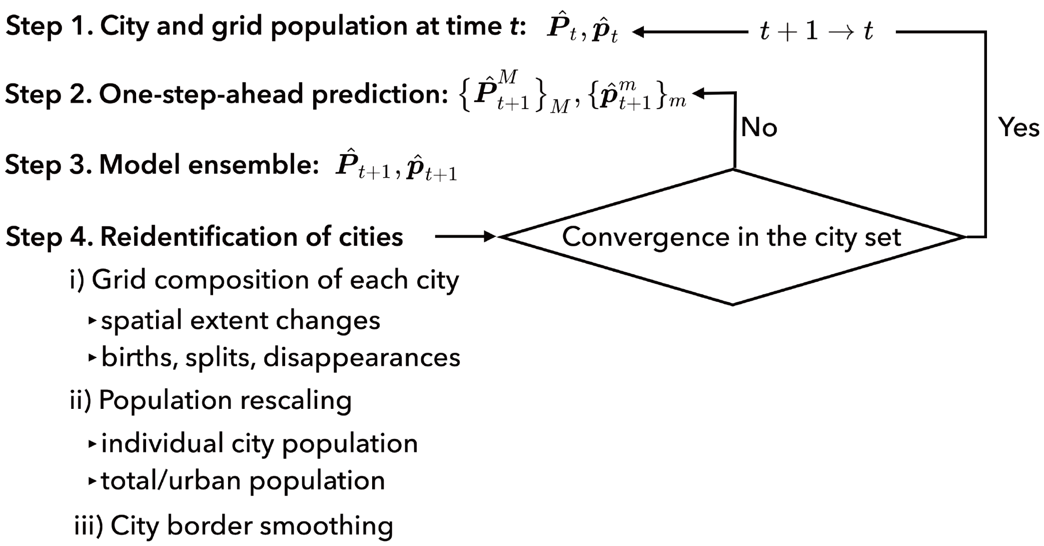

Figure 9. The projection procedure

4.5 Model validation and model selection

Our goal is to make a long-term projection of the geographic distribution of the population, based on the trends of population decline and reduction of distance frictions that have become pronounced only in recent decades. Since it is particularly important to extrapolate the new trends that threaten the regional economy, our training time series data are necessarily short.

In this section, we show that it is particularly important to focus on city-level factors in order to make a reasonable projection of population size not only at the city level, but also at the grid level.

Consider predicting the grid- or city-level population distribution in 2020 by training the model on 1970–2015 data. Not surprisingly, the population size of each grid and city does not change much over five years, so the model fit in terms of size is nearly perfect. However, the population growth rates of the grids/cities are not necessarily correctly predicted.

Figure 10 shows the overidentification of the model regarding population growth rates at the grid level under three choices of models. Panel A shows the case where only the grid-level time series models are used. In panel B, the city-level time series models are added to the grid-level models, and in panel C, the PL model is also added. The 95% confidence intervals are quite tight in all cases.

Note that the proportion of correct signs for predicted population growth is significantly improved (from 45% to 57%) when city-level time series models are added. Thus, even at the grid level, city-level factors appear to be important in explaining population growth.

Not surprisingly, adding the PL model does not improve the model fit much in the short-run. However, it is important to confirm that the addition of the PL model does not worsen the prediction. Since the PL model is intended to simulate the long-term change in power law coefficients, its short-term role is limited.

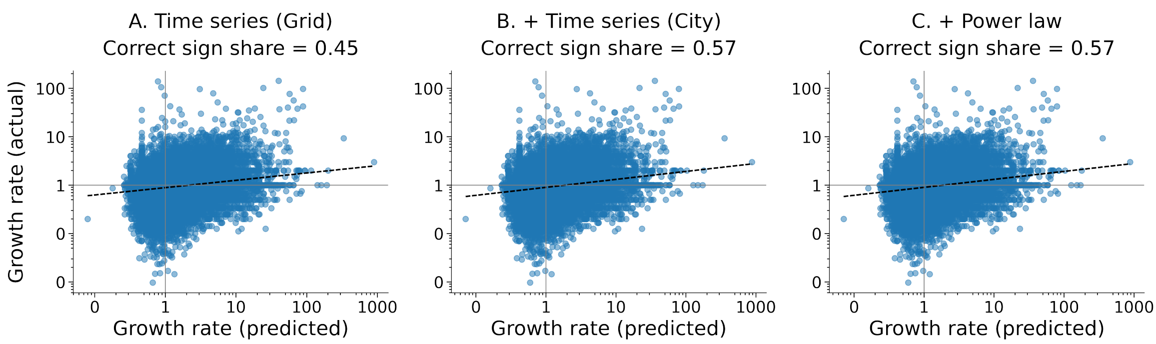

Figure 10. Model performance for predicting population growth in grids

Notes: (A) The grid-level population in 2020 is predicted from the 1970–2015 data using the grid-level time-series models in Section 4.3. (B) The result after adding the city-level time-series models in Section 4.2. (C) The result after adding the PL model in Section 4.1. The dashed line is the fitted linear regression line, and the shaded area is its 95% confidence interval (the confidence bands are too narrow to visualize).

Figure 11 shows the model fit with respect to the population growth rate at the city level. The model choices in the panels are the same as in Figure 10. Panel A shows that the city-level population growth rates are not correctly predicted by the grid-level time-series models alone, as the actual and predicted growth rates are negatively correlated. In panel B, the model performance improves significantly after adding the city-level time-series model. The correlation between actual and predicted growth rates has the correct sign, and the proportion of correct signs of predicted city growth improves significantly from 52% to 82%. In panel C, the addition of the PL model does not worsen the model fit.

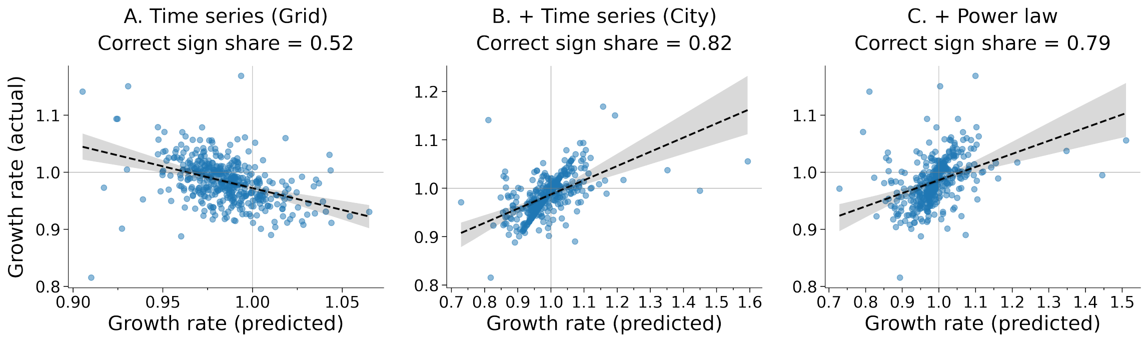

Figure 11. Model performance for predicting population growth in cities

Notes: (A) The city-level population in 2020 is predicted from the 1970–2015 data using the grid-level time-series models in Section 4.3. (B) The result after adding the city-level time-series models in Section 4.2. (C) The result after adding the PL model in Section 4.1. The dashed line is the fitted linear regression line, and the shaded area is its 95% confidence interval.

Figure 12 illustrates the effectiveness of the city-level models. The figure compares the actual and predicted growth rates of the grid population in the Tokyo UA for the prediction of the grid population in 2020 from the 1970–2015 data. Panel A shows that the population growth around Tokyo's central business district (CBD) is underestimated when only grid-level models are used. Panel B shows the result when the city-level time-series models are added. Although population growth at the core of the CBD is still underestimated by the models, the fit of the model is significantly improved. Panel C shows the result when the PL model is also added, which essentially does not change the results of Panel B. We can see that the grid population is strongly influenced by the city-level factors.

Although the PL model does not affect the short-term forecast when time-series models are included at the city level, it is still selected by a significant number of cities. Figure 13 shows the frequency distribution of the weights, W_u^{PL} and W_u^{TS}, for the PL and TS models in the city-level model ensemble given by eq. (10). On average, the PL weight is 0.37. Thus, on average, 37% of the comparative static effect, which changes the power law coefficient for the city size distribution, will influence the growth process of individual cities.

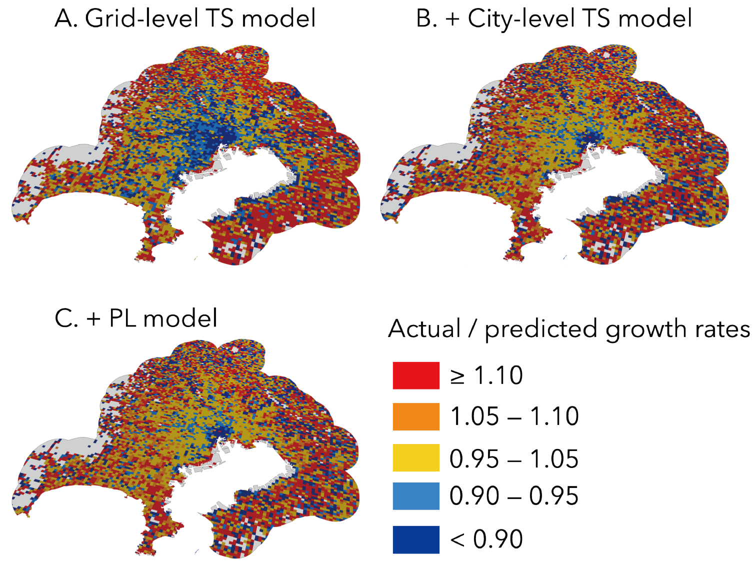

Figure 12. Model performance for predicting the grid population growth in Tokyo

Notes: The ratio of the actual and predicted growth rates of the grid population in Tokyo UA for the prediction of the 2020 population from the 1970–2015 data. (A) shows the result when only the grid-level time-series models in Section 4.3 are used. (B) adds the city-level time-series models in Section 4.2, and (C) further adds the PL model in Section 4.1.

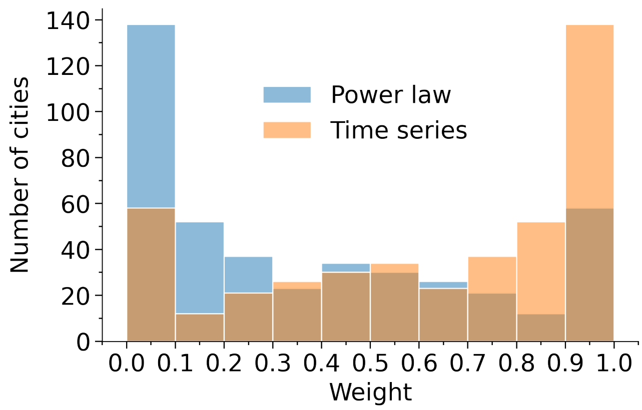

Figure 13. Selection between the PL and time-series models at the city level

Notes: The histogram shows the frequency of cities that adopted the PL and TS models with a given pair of weights, W_u^{PL} and W_u^{TS}, in eq. (10) to predict city sizes in 2020 from the 1970–2015 data. The average values of W_u^{PL} and W_u^{TS} across all cities u are 0.37 and 0.63, respectively.

5 Baseline scenario

In this section, we present the result of our projection under the baseline scenario for Japan's population growth to 2200. We begin by summarizing the evolution of the number of cities and the distribution of city sizes in Section 5.1, and show a broad picture of the projected regional variation in future population growth in Section 5.2. In Section 5.3, we look at the rise and fall of individual cities behind the regional variation in population growth, and discuss the relationship between city growth and aging. In

Section 5.4 we show how the spatial frequency of the focal cities will change in the future. Their future geographic distribution suggests the geographic extent of future regional coordination, replacing prefectures and municipalities. We take a closer look at the depopulating rural regions in Section 5.6, and how the population distribution in large cities will change in Section 5.7. Finally, we calculate the impact of population decline on land prices in Section 5.8.

5.1 Evolution of city counts and city size distribution

The baseline scenario assumes that the fertility rate of 1.36 in 2020 will persist in the future,[5] while the pessimistic and optimistic scenarios assumes the fertility rate of 1.13 and 1.64, respectively, will persist in the future. Figure 14 shows the future number of cities predicted in these three scenarios. In the baseline scenario, the number of cities decreases by 18%, 24%, and 26% every 50 years from 2020 to 2070, 2070 to 2120, and 2120 to 2170, respectively.

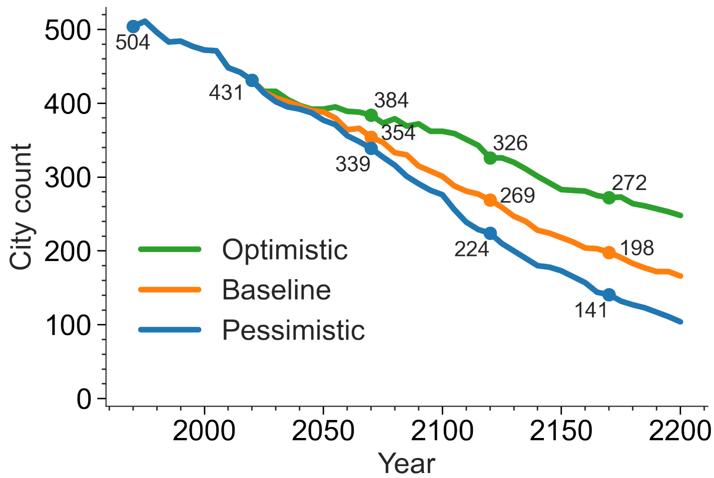

Figure 14. Predicted numbers of cities

Notes: The realized number of cities in years 1970–2020, and the predicted number of cities in years 2025–2200 under the three alternative scenarios of Japan's population projection (Fig. 8A).

Figure 15A shows the observed city-size distributions in 2020 together with the projected ones in 2070, 2120, and 2170, under the baseline scenario. The power coefficient B_t increased from -1.30 to -1.19 from 2020 to 2120, despite the PL model predicts a decrease in B_t. This is mainly due to the fact that large cities are divided into smaller pieces as the total population decreases. However, the concentration towards largest cities continues, as Tokyo's population share in all cities increases from 34% in 2020 to 37% in 2120.

[5]This assumption may be too optimistic, as the fertility rate decreased to 1.30 and to 1.26 in 2021 and 2022, respectively (Ministry of Health, Labour and Welfare of Japan, 2022).

Figure 15B supplements Figure 7 with the predicted average and maximum population density and area of cities for 2025-2200. The population density in cities is projected to decrease much faster than the area of cities, i.e., the flattening of cities will continue steadily, reflecting the projected trend of decreasing distance frictions. Specifically, the average population density in a city will decrease by an average of 6.1% from 2020 to 2070 and 12.2% from 2020 to 2120, while the area of a city will increase by 4.7% from 2020 to 2070 and 5.1% from 2020 to 2120. The population decline associated with the flattening of cities suggests significant changes in housing demand and land price, as will be discussed in Section 5.8.

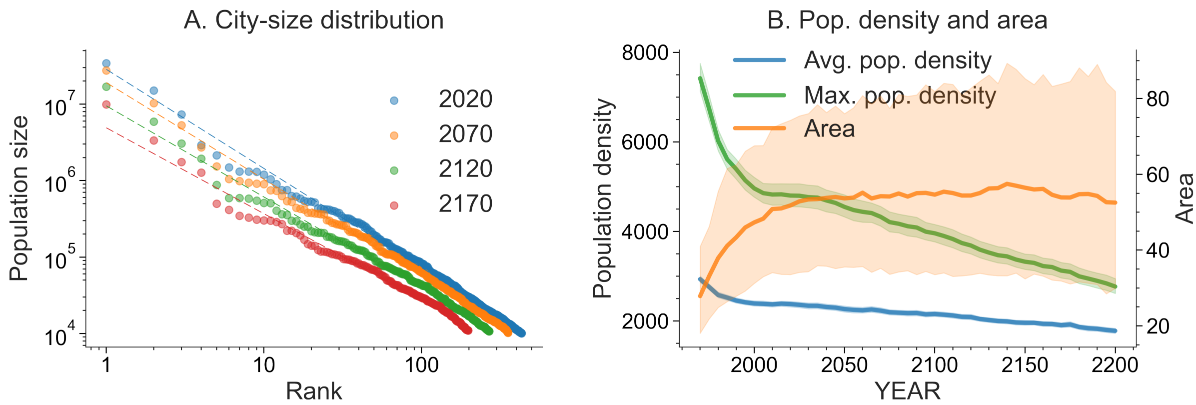

Figure 15. Predicted city-size distributions, average and maximum population density and area of cities (baseline)

5.2 Regional variation in city growth

To get a broad picture of the future organization of Japan's regional economy, we look at the projected evolution of the top five cities in 2020 in Figure 16A. While these five cities will still be the top five by 2200, only Tokyo and Fukuoka will continue to grow in population share. It is in line with the implication of the theory of economic agglomeration that fewer, larger, and more distant cities will remain under decreasing transportation costs (Akamatsu et al., 2023). In particular, Osaka and Nagoya will become too close to Tokyo to maintain their population size.

Figure 16B shows the evolution of population shares in the seven traditional regions shown in Figure 17. There is a clear dichotomy between the east and west sides of Tokyo. In the east of Tokyo, both Hokkaido and Tohoku are expected to decline faster than the western regions. These variations are picked up by the time-series models, which take into account city and grid specific factors. We will see in Section 5.5 that rapid aging in the eastern regions may have accelerated the depopulation of these regions.

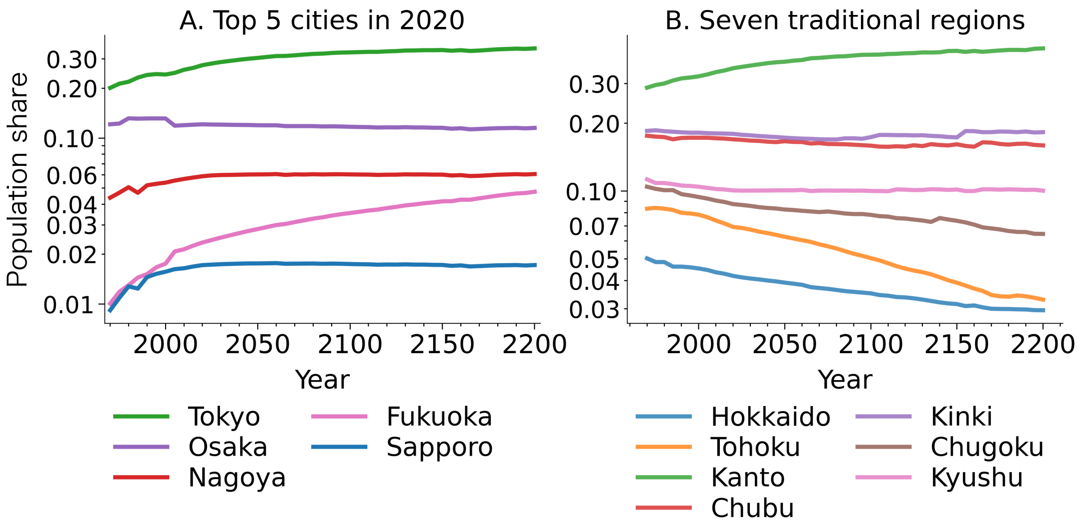

Figure 16. Predicted population shares of the top five cities and traditional seven regions

Notes: (A) The projected shares of the 5 largest cities in Japan as of 2020 in the total population of Japan. (B) The projected shares of the traditional seven regions (Fig. 17) in the total population of Japan.

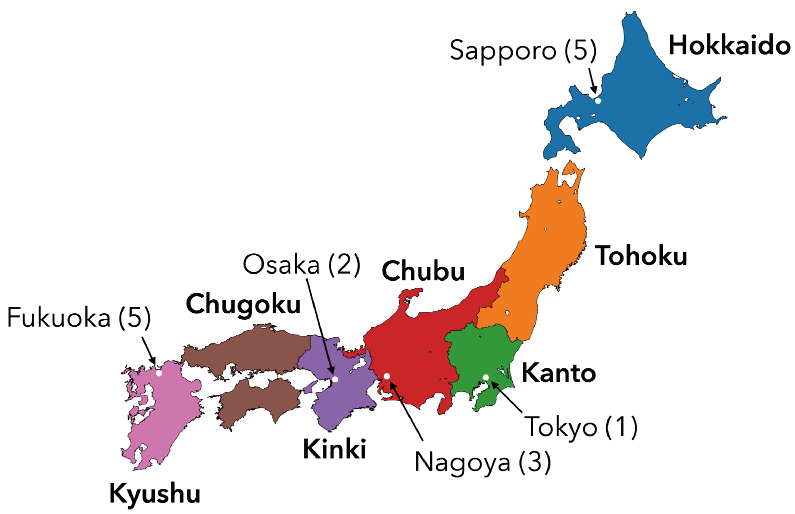

Figure 17. Traditional seven regions and the locations of top 5 cities in 2020

Notes: Each of the seven regions are named as follows. Blue: Hokkaido, Orange: Tohoku, Green: Kanto, Red: Chubu, Purple: Kinki, Brown: Chugoku, Lavender: Kyushu. The 5 largest cities in 2020 are shown, with the numbers in parentheses indicating their ranking in terms of population size.

5.3 Rise and fall of individual cities

We now compare the rise and fall of individual cities in the past half century and in the coming century. Figure 18 shows the growth of the population share of individual cities between 1970 and 2000. During this period, most cities increased their share, except for the old industrial cities such as Kitakyushu and Shizuoka. Since it covers both the high-growth period (1970–1975) and the bubble era (1980–1990) in Japan, this was the time when cities were particularly attractive, leading to rapid urbanization.

Figure 19 shows the growth of the population shares of cities in the period 2000–2020. Most of the cities east of Tokyo, except those along the high-speed rail lines (see Fig. 4A), began to decline. West of Tokyo, Osaka began to decline. In addition to the bullet train line connecting all major western cities between Fukuoka and Tokyo in 1975, frequent express trains, called the Nozomi Express, were introduced between Fukuoka and Tokyo in 1992, bringing these cities closer to Tokyo economically. Especially the improved connections between Tokyo and Osaka may have pushed Osaka into Tokyo's agglomeration shadow (e.g., Fujita and Krugman, 1995). Osaka has been in decline since 2000.

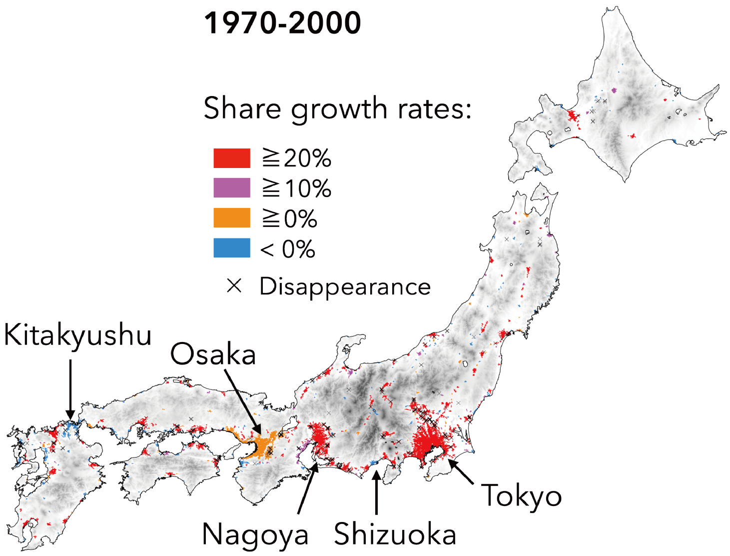

Figure 18. Growth in population share of cities: 1970–2000

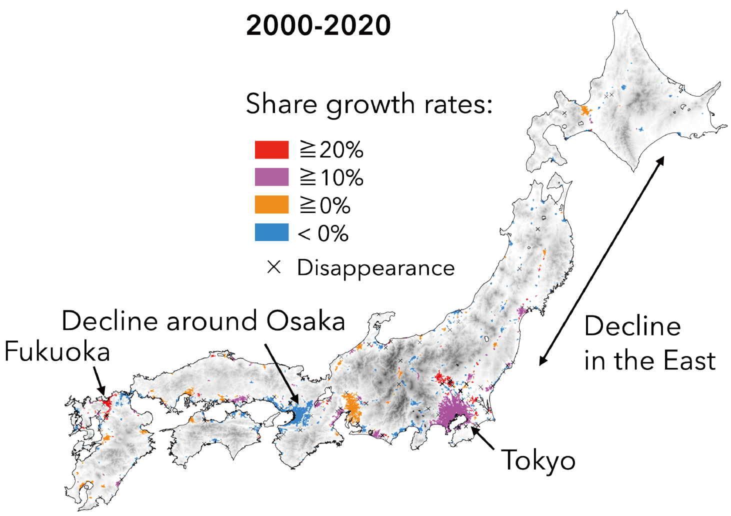

Figure 19. Population share growth of cities: 2000–2020

Figure 20 shows the evolution of cities in the period 2020–2070. The cities east of

Tokyo continue to shrink and disappear, even along the bullet train lines. West of Tokyo, smaller cities between Nagoya and Tokyo and around Osaka begin to decline. Large cities such as Hiroshima and Okayama along the bullet train lines west of Tokyo continue to grow in population share by absorbing population from the declining cities around them.

Figure 21 shows the evolution in the period 2070–2120. The area between Osaka and Tokyo is mostly shrinking, including the third largest Nagoya, and the region east of Tokyo and the northern coast of the main island is shrinking, except for a few large cities such as Sendai and Kanazawa.

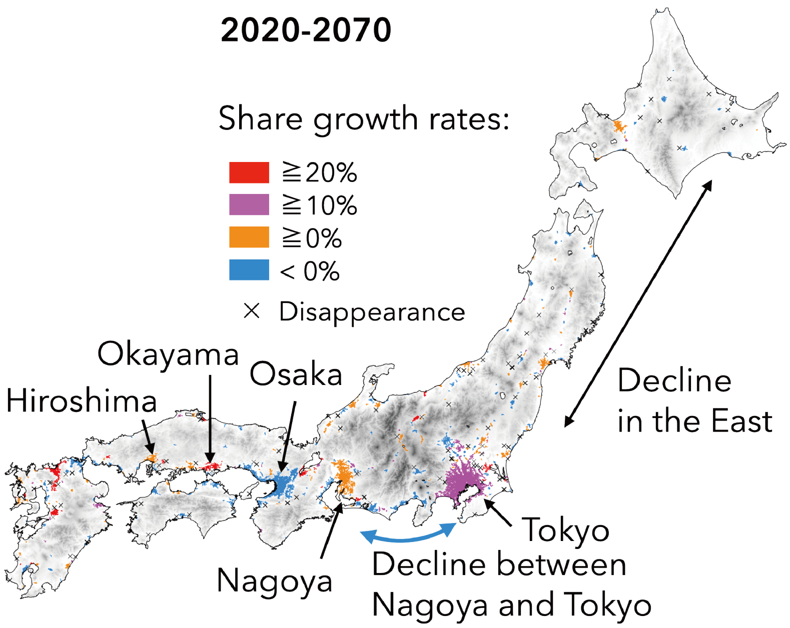

Figure 20. Population share growth of cities: 2020–2070

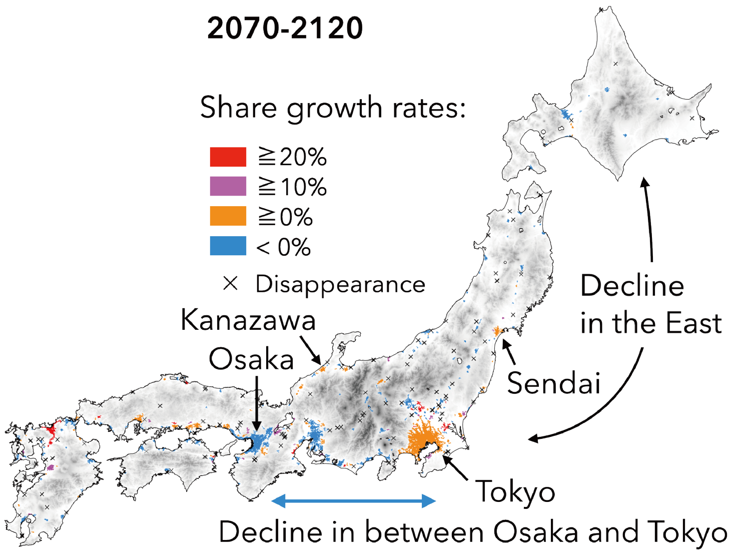

Figure 21. Growth in urban population share: 2070–2120

By 2170, only Tokyo, Fukuoka, and Hiroshima among the 10 largest cities manage to increase their population share, as shown in Figure 22. Some small growing cities that split off from nearby major cities, such as those around Nagoya, collect population from the surrounding declining area, but may not have their own growth drivers. Cities east of Tokyo, Shikoku Island, and the southern half of Kyushu Island appear to be emptying out.

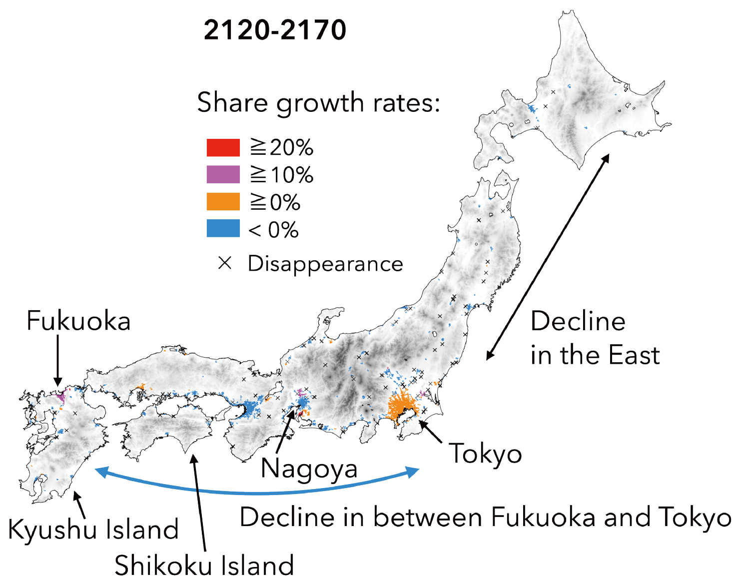

Figure 22. Growth in population share of cities: 2120–2170

5.4 Geographic distribution of focal cities

In this section, we present the future geographic distribution of *focal cities* that are large cities expected to play the role of economic centers in their surrounding regions. We consider cities in three size classes, those with at least 100,000, 500,000, and 1 million inhabitants. In particular, in the third *National Spatial Strategy* approved by the Japanese government in 2023, the minimum threshold of population size is considered to be 100,000 for a *Life Zone* to maintain basic infrastructure and functions for living, such as public schools, basic medical and commercial facilities.

Theory suggests that these focal cities will be fewer and farther apart as the country's population declines and distance frictions diminish. In order to design regional development policies, it is crucial to know which of the current focal cities will be viable in the future. Therefore, our aim in this section is to quantitatively predict their future geographic distribution.

In 2020, Japan, with a total population of 124 million, has 83 cities with at least 100,000 inhabitants and 21 cities with at least 500,000 inhabitants, as shown in Figure 23A and B, respectively. To get a sense of the distance between them, the Voronoi partitions of the land area with respect to these cities are shown in the map.[6] While cities are more densely clustered in western Japan, they are spread throughout the country. Cities of at least 500,000 inhabitants are similarly distributed throughout the country, except that they are more dispersed than those of at least 100,000 inhabitants, so that each of their Voronoi cells contains three or four cities of at least 100,000 inhabitants.

Since there are 46 prefectures on the map shown in the figure, at present, each of the focal cities of at least 100,000 inhabitants serves roughly half the size of a prefecture, while that of at least 500,000 inhabitants serves roughly the size of two prefectures.

After 50 years in 2070, Japan's population is expected to decline by a third to 86 million. The number of cities with at least 100,000 and 500,000 inhabitants will decrease to 70 and 15, respectively. The remaining cities are more dispersed.

One hundred years later, in 2120, Japan's total population is projected to be approximately 40% that of 2020 (Fig. 25). The number of cities with at least 100,000 and 500,000 inhabitants will fall to 49 and 11, respectively, and will again be more widely dispersed. This compares to 42 and 6, respectively, in the pessimistic scenario.

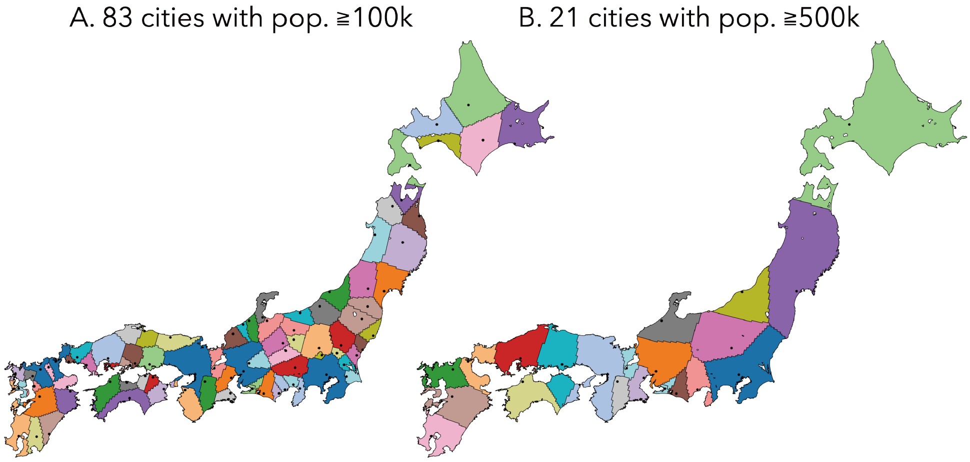

Figure 23. Geographic distribution of focal cities in 2020

Notes: In (A) and (B), the black dots indicate the location of cities with at least 100,000 and 500,000 inhabitants, respectively, in 2020. The cells on the map are those of the Voronoi partition of the country with respect to these cities.

[6]In the Voronoi partition, each 1-km grid cell is assigned to the nearest of the cities with populations of at least 100,000 and 500,000 in Panels A and B, respectively.

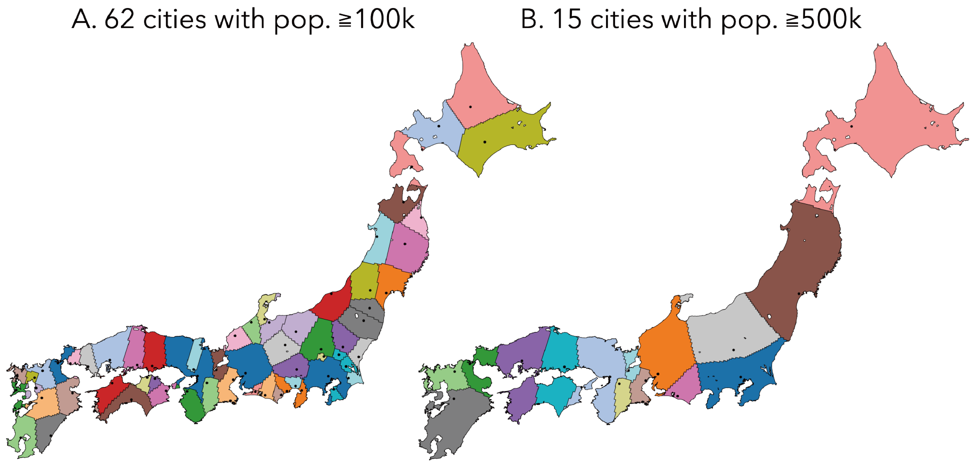

Figure 24. Geographic distribution of focal cities in 2070

Notes: In (A) and (B), the black dots indicate the location of cities with at least 100,000 and 500,000 inhabitants, respectively, in 2070. The cells on the map are those of the Voronoi partition of the country with respect to these cities.

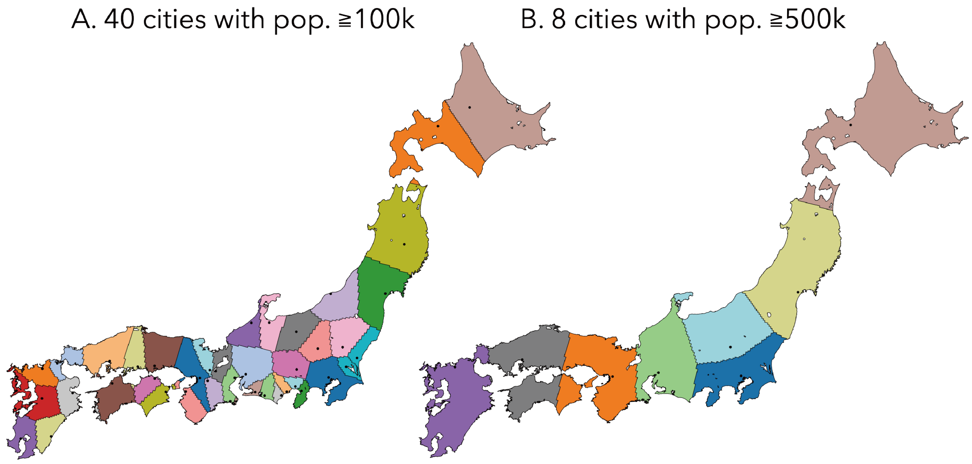

Figure 25. Geographic distribution of focal cities in 2120

Notes: In (A) and (B), the black dots indicate the location of cities with at least 100,000 and 500,000 inhabitants, respectively, in 2120. The cells on the map are those of the Voronoi partition of the country with respect to these cities.

Finally, Figure 26 shows the changes in the location of cities with at least 1 million inhabitants. There are 11 in 2020, decreasing to 6 in 2070 and 4 in 2120. Again, they will be further apart from each other, while concentrating in the west.

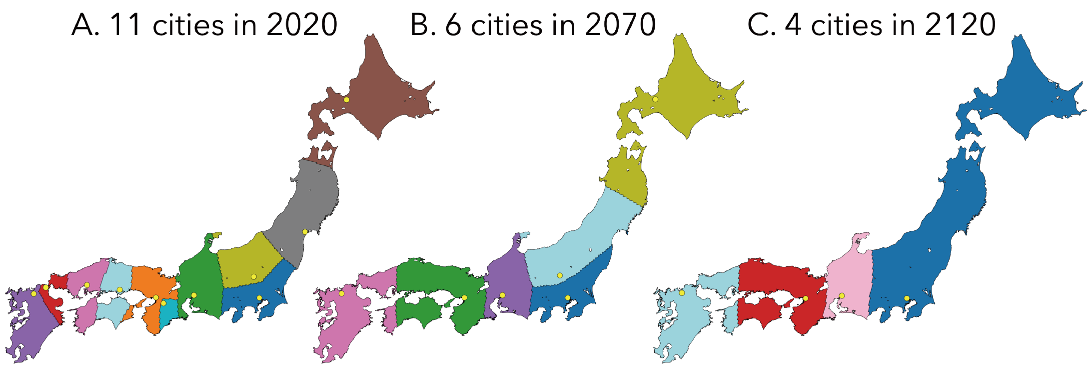

Figure 26. Geographic distribution of million cities

Notes: In (A), (B), and (C), the yellow dots indicate the location of cities with at least 1 million inhabitants in 2020, 2070, and 2120, respectively. The cells on the map are those of the Voronoi partition of the country with respect to these cities.

5.5 Aging and city growth

The population decline of Japan is associated with aging and the decreasing fertility rate. Figure 27 indicates the rapidly increasing share of the population aged 65 or older, and the rapidly decreasing share of the population aged 14 or younger. The share of population aged 65 or older will increase from 28% in 2020 to 55% in 2120, whereas that of population aged 14 or younger will decrease from 12% to 8% in the same period.

In addition, the age composition of the population is projected to vary across regions according to the National Institute for Environmental Studies, Japan (NIES) (2021). Figure 28 shows the regional variation in the *dependency ratio*, which is the ratio of the population under the age of 15 or over the age of 64 to the *working age population* between the ages of 15 and 64 in every 50 years during the period 2020-2120. Note that eastern Japan appears to age more rapidly after 2070, which is consistent with the rapid decline of cities in the region discussed in Section 5.3. Although our forecasting model does not explicitly incorporate the aging factors, our time-series models should have captured their effect on the growth process at both the grid and city levels.

Figure 29 confirms that cities with a higher rate of aging and a lower proportion of children tend to have lower or negative population growth.

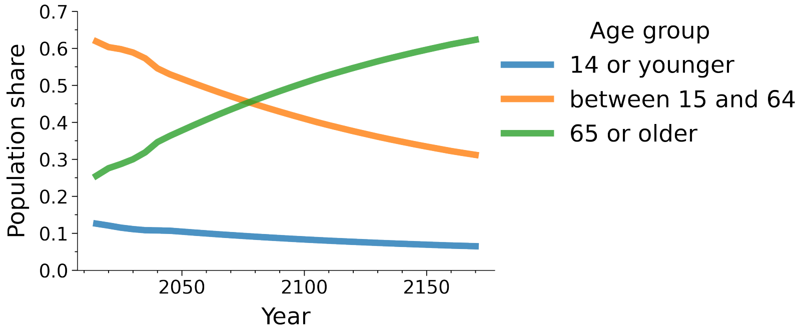

Figure 27. Forecasts of age-group decomposition of total population in Japan

Notes: The projection of age-group decomposition was obtained for 2015–2045 from the NIES (2021). We extraporated the projection to 2200 as follows: (1) the population share aged 14 or under is projected by assuming log-linear function of time; (2) the population share aged 65 or older is projected by using the same model; (3) the population share aged between 15 and 64 is projected by subtracting these two share from 1.0.

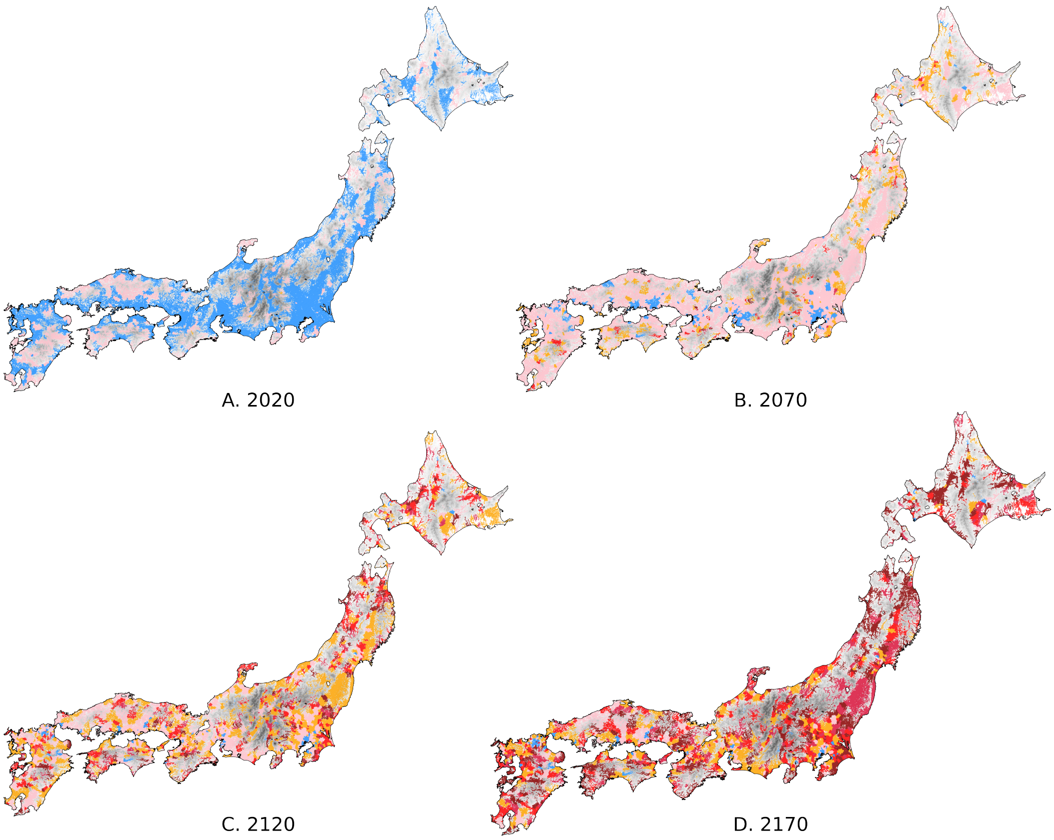

Figure 28. Forecasts of dependency ratio at the grid level in Japan

Notes: The projection of the age group decomposition was obtained for 2015–2045 from the NIES (2021). We extrapolated the projection to 2200. We then matched each grid to a municipality and assign the age group shares in the municipality to the grid. The dependency ratio is calculated as the ratio of the population younger than 15 or older than 64 to the population between 15 and 64. (A–D) show the dependency ratios, D, at the grid level in the years 2020, 2070, 2120 and 2170, respectively. Blue: $D \leq 1$, Pink: $1 < D \leq 2$, Orange: $2 < D \leq 3$, Red: $3 < D \leq 4$, Crimson: $4 < D \leq 5$, Dark red: $D > 5$. The grayscale colors indicate geographic altitude, where a darker color means higher.

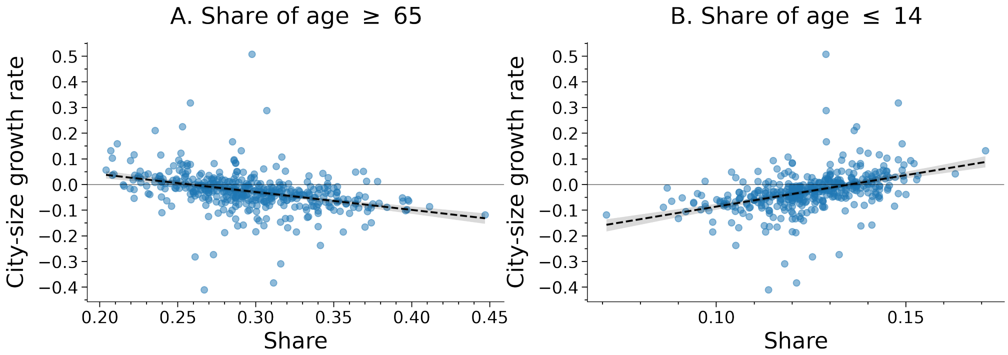

Figure 29. Age-group share and city-size growth

Notes: (A) A city's 5-year population growth rate versus the share of the city's population aged 65 or older in years 2015,2020,...,2195. (B) A similar plot with the horizontal axis indicating the share of the city's population aged 14 or younger. The dashed line in each panel is the fitted regression line with a 95% confidence interval as the shaded band.

5.6 Fate of rural regions

In this section, we take a closer look at the fate of rural regions by focusing on two typical cases.

Depopulating peripheral regions

Kochi prefecture, shown on the map in Figure 30, is a typical peripheral prefecture, far from major railways and highways, and facing rapid depopulation. The population of this prefecture is expected to decline by 78% from 690,774 to 151,109 between 2020 and 2120, while the country's population is expected to decline by 59% over the same period. The proportion of the population over the age of 64 in this prefecture will increase from 35% to 61% between 2020 and 2120, while that of the country will increase from 29% to 55%. The graph in Figure 30 shows the evolution of the population size of cities in Kochi prefecture.

The prefecture defines a naturally coherent region surrounded by mountains and organized around the largest city, Kochi as shown in Figure 31. The figure shows the locations of cities that existed in 1970 and 2020, as well as those predicted to exist in 2070 and 2120.

In 1970, there were seven cities scattered along the coastal areas of the prefecture. By 2020, all the outlying cities except Shimanto have disappeared, and the cities are clustered around the largest city, Kochi. By 2070, the only outlying city, Shimanto, will disappear, and by 2120, only Kochi will remain. The population of Kochi city will shrink from 284,237 in 2020 to just over 100,000 in 2120 (by 64%). Thus, Kochi as a prefecture will face an existential crisis. Prefectures in southern Kyushu, along the northern coast of the main island, and in eastern Japan are expected to have a similar future.

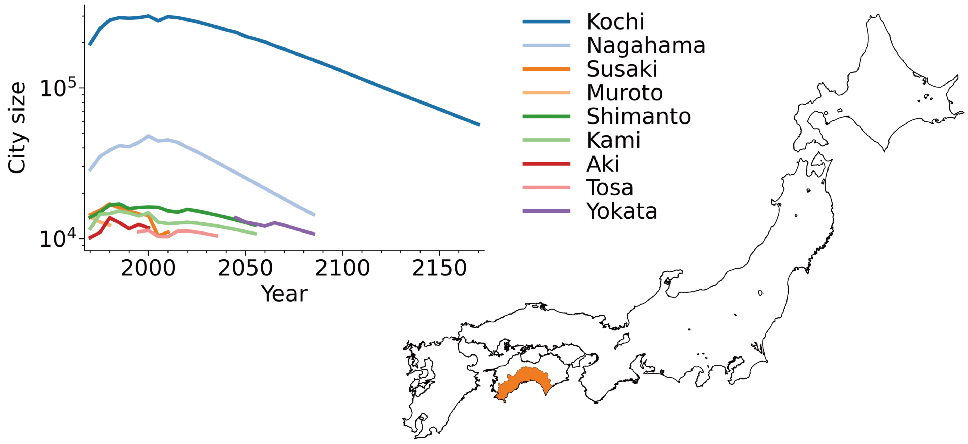

Figure 30. Projection of city sizes in Kochi prefecture

Notes: The graph shows the evolution of the population size of the cities during the period 1970–2200 in the Kochi prefecture, whose location is indicated on the map. Only the cities that existed for at least 10 consecutive years are shown in the graph.

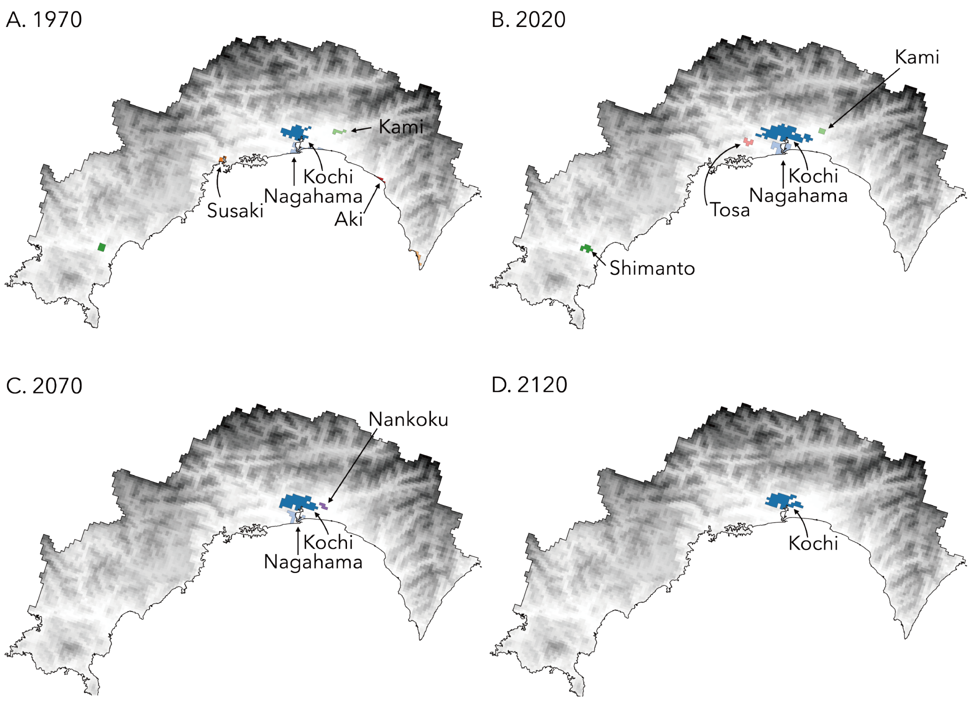

Figure 31. Cities in Kochi prefecture

Notes: (A–D) show the map of cities that exist in Kochi prefecture in 1970, 2020, 2070, and 2120, respectively.

Regions around major cities

Next, we consider the case of Okayama prefecture, shown in Figure 32. This prefecture contains the 11th largest city, Okayama, in 2020. Although most of the outlying cities will disappear by 2120 (Fig. 33) as in the case of Kochi prefecture, Okayama prefecture will better maintain its population, as its population of 1,040,452 in 2020 will decline by only 44% to about 580,000 in 2120, compared to 59% for the country.

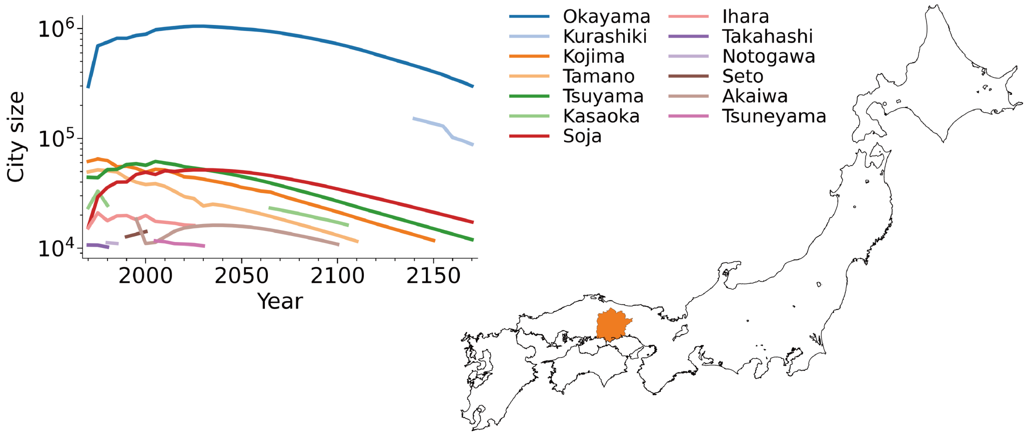

Figure 32. Projection of city sizes in Okayama prefecture

Notes: The graph shows the evolution of the population size of the cities during the period 1970–2200 in Okayama prefecture, whose location is indicated on the map. Only the cities that existed for at least 10 consecutive years are shown in the graph.

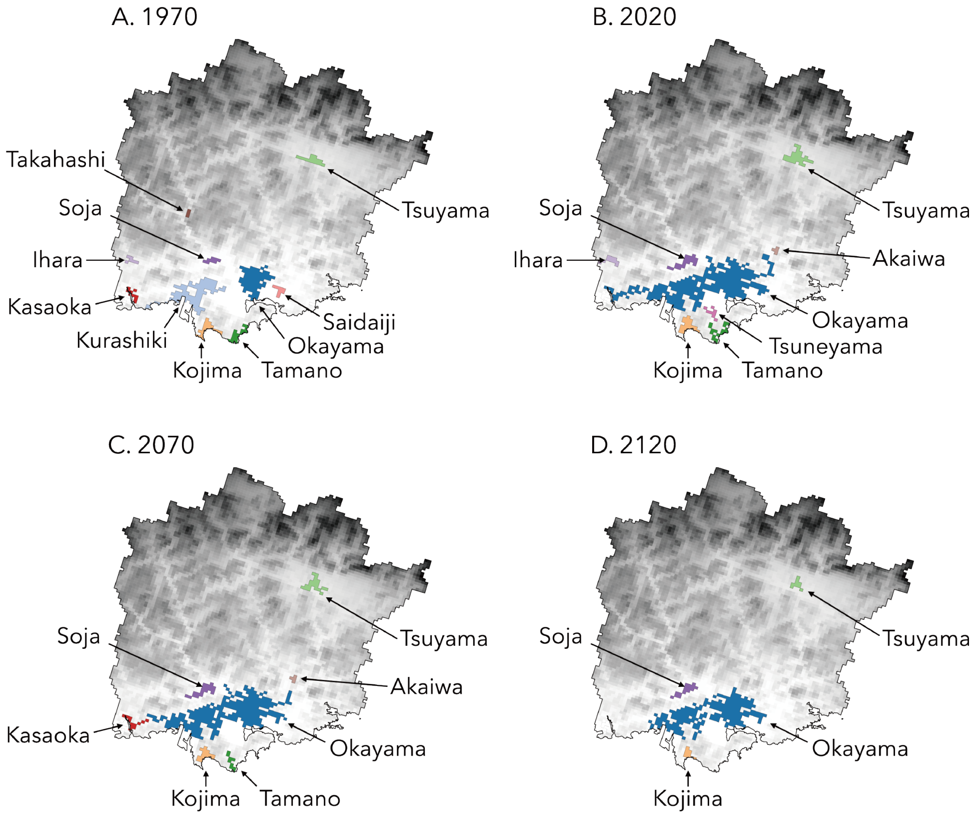

Figure 33. Cities in Okayama prefecture

Notes: (A–D) show the map of cities that exist in Okayama prefecture in 1970, 2020, 2070, and 2120, respectively.

The prefecture's population will decline from 1,885,645 in 2020 to about 768,000 in 2120 (a decline of 59%). While the prefecture will be more dominated by the largest

Okayama (Fig. 32), it will maintain a reasonable population for a prefecture.

The coastal prefectures between Tokyo and Fukuoka will follow a similar path, with the major cities of these prefectures absorbing the population of the small, depopulated surrounding cities. Although the progress is slower than in peripheral prefectures such as Kochi, these coastal prefectures are still in decline compared to Tokyo and Fukuoka.

5.7 Inside the large cities

What will happen to the internal structure of the remaining cities? In our baseline scenario, we assume that transportation costs will continue the declining trend of the past 50 years and that total population will also decline at the projected rate. Theory suggests that the population of each city will decline, while the geographic distribution of the population within the city will flatten. In this section, we take a closer look at the interior of the top 4 cities in 2020.

Tokyo

Figure 34 shows the change in the geographic distribution of Tokyo's population from 1970 to 2120. Between 1970 and 2020, Tokyo's population increased substantially by 67% from 205 million to 342 million, compared to the country's population increase of 22%. However, the maximum population density decreased by 20% from 40,680 to 32,706, while the area increased by 47%. Thus, Tokyo has clearly flattened out despite its population growth.

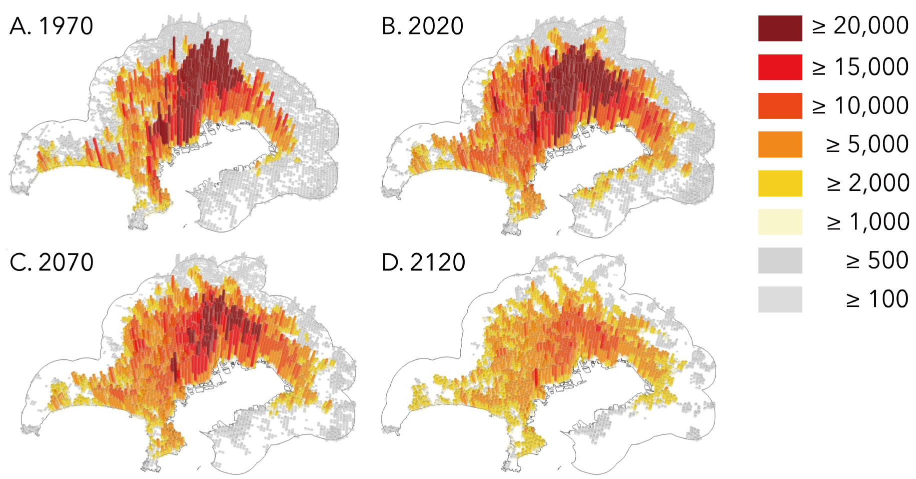

Figure 34. Geographical distribution of population in Tokyo UA

Notes: (A–D) show the grid population around Tokyo UA in 1970, 2020, 2070, and 2120, respectively, under the baseline scenario for the Japan's population projection.

The geographic distribution of Tokyo's population will continue to flatten from 2020 to 2070 and 2120. The population (maximum population density) in Tokyo is expected to decrease to 276 million (25,545) in 2070, and then to 170 million (16,110) in 2120, halving between 2020 and 2120. Meanwhile, the area will only decrease by 16%. Thus, Tokyo will continue to flatten out as its population decreases in the coming century, indicating the influence of the decrease in distance frictions over time.

Osaka

Let us take a closer look at the case of the second largest city, Osaka, shown in Fig. 35.

Between 1970 and 2020, Osaka's population increased by 22% from 124 million to 151 million, the same as the country's population growth. Thus, Osaka shows signs of losing its appeal as a major metropolis relative to Tokyo. Otherwise, it shares the trend of flattening out with Tokyo, as the maximum population density decreased by 29% from 40,635 to 29,033, while the area increased by 30%.

The geographical distribution of Osaka's population will continue to flatten from 2020 to 2070 and 2120. The population (the maximum population density) in Osaka is expected to decrease to 103 million (20,165) in 2070 and then to 59 million (12,428) in 2120, a decrease of 61% (57%) between 2020 and 2120. Meanwhile, the area will decrease by only 25%.

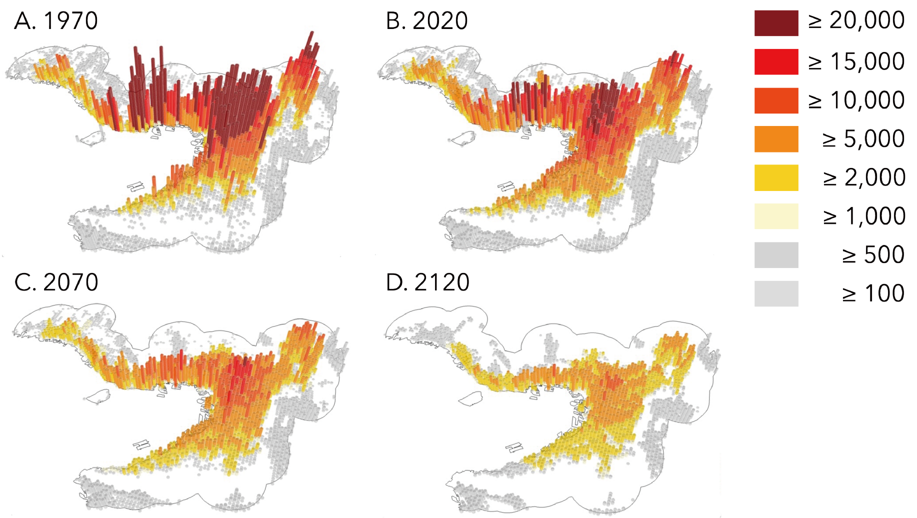

Figure 35. Geographical distribution of the population in Osaka, UA

Notes: (A–D) show the grid population around Osaka UA in 1970, 2020, 2070, and 2120, respectively, under the baseline scenario for the Japan's population projection.

Nagoya

Nagoya's population density is significantly lower than that of Tokyo and Osaka at all times during the study period. This is due to Nagoya's specific postwar urban planning to maintain a low population density. Otherwise, Nagoya shows a similar declining trend as Osaka in the future.

Between 1970 and 2020, Nagoya's population increased by 64% from 4.46 million to 7.32 million, while the maximum population density decreased by 28% from 23,925 to 18,054, and the area increased by 30%. Thus, over the past half-century, Nagoya has experienced population growth similar to that of Tokyo, which is associated with flattening within a city. However, Nagoya's projected future is more like Osaka's than Tokyo's. The population (the maximum population density) in Nagoya is expected to decrease to 5.29 million (12,058) in 2070, and then to 3.06 million (8,120) in 2120; that is, it will decrease by 58% (55%) between 2020 and 2120. Meanwhile, the area will decrease by only 37%.

Note also that in 1970 there were several small distinct peaks of population agglomeration in the outskirts of Nagoya. But they almost disappeared by 2020, being absorbed into Nagoya. By 2120, Nagoya is almost a monocentric city.

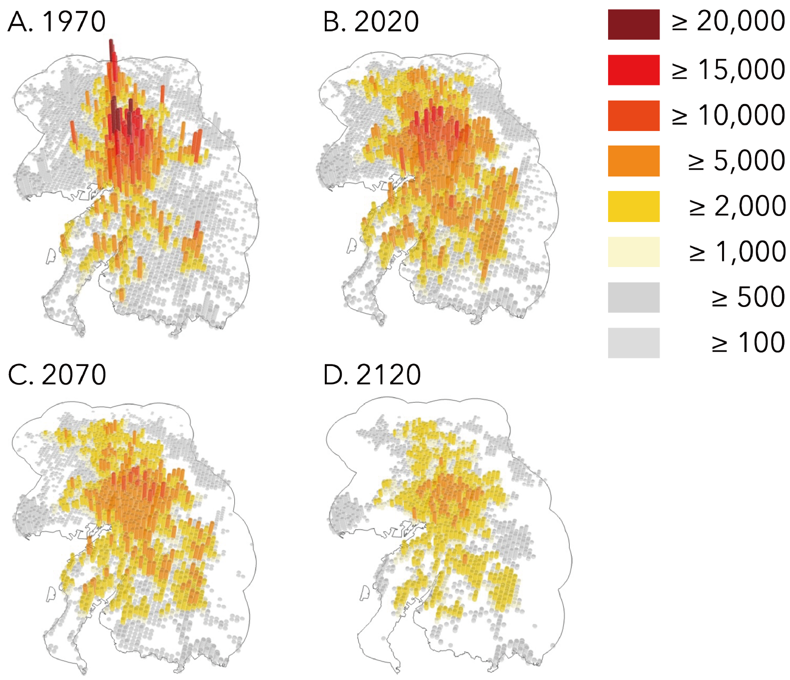

Figure 36. Geographical distribution of population in Nagoya UA

Notes: (A–D) show the grid population around Nagoya UA in 1970, 2020, 2070, and 2120, respectively, under the baseline scenario for the Japan's population projection.

Fukuoka

As we have seen in Section 5.3, Fukuoka is the growth pole of Japan in the coming century, next to Tokyo. Since the opening of the bullet train line to Tokyo in 1975, Fukuoka has continued to grow in both area and population (Fig. 37A,B). Between 1970 and 2020, its population grew 184% from 19,380 to 28,306, while its area grew 46%. Unlike Osaka and Nagoya, Fukuoka will continue to maintain a high density in the CBD. In 2120, Fukuoka's maximum population density is expected to reach 18,759, which is higher than Tokyo's 16,110, while the average population densities of these cities are similar at 4,311 and 4,847, respectively.

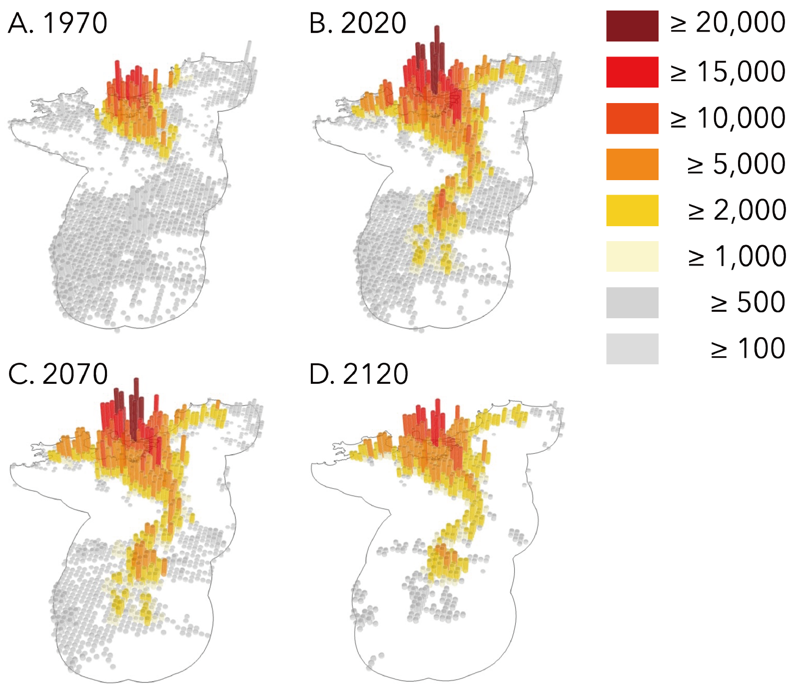

Figure 37. Geographical distribution of population in Fukuoka UA

Notes: (A–D) show the grid population around Fukuoka UA in 1970, 2020, 2070, and 2120, respectively, under the baseline scenario for the Japan's population projection.

5.8 Land price

The declining population will naturally result in a decrease in the price of the land. Using the predicted geographic distribution of the population in the country, and the point data for the official land price in 1985–2020 (Ministry of Land, Infrastructure, Transport, and Tourism of Japan, 1985–2020), we predict the geographic distribution of the land price in the future.[7]

To this end, we assume that the price of residential land $L_{i',t}$ evaluated at site i' in year t is assumed to obey the following semiparametric regression model (see Wood, 2017):

$$\ln L_{i',t} = \sum_{k=1}^{K} X_{i',t,k}\beta_k + \beta_{u(i',t)} + f_{el}(Z_{i',el}) + f_{sp}(\mathbf{Z}_{i',sp}) + \epsilon^L_{i't'}, \qquad \epsilon^L_{i',t} \sim N(0, \sigma^2_L) \tag{13}$$

where $X_{i',t,k}$ is the k-th covariate assuming a linear association with $L_{i',t}$ and β_k is the coefficient. The covariates include the logarithm of population density in the 1 km

[7]For 1985–2020, there are 25,000–49,700 points at which land prices have been officially evaluated on January 1st every year. We use the data on every five years between 1985 and 2020 that match our gridded population data.

grid that contains site i' and logarithm of the average population densities in the adjacent grids. Their log-linear functions assume that the incremental impact per unit population declines as population increases. $\beta_{u(i',t)}$ represents the fixed effect of the city u containing site i' in year t.

In addition, elevation $Z_{i',t,el}$ and geographic coordinates $\mathbf{Z}_{i',t,sp}$ are included to improve prediction accuracy. [8] A thin-plate spline $f_{el}(Z_{i',t,el})$ is used to estimate the nonlinear influence of elevation on land price, while a low-rank Gaussian process $f_{sp}(\mathbf{Z}_{i',t,sp})$, widely used in spatial statistical modeling (e.g., Banerjee et al., 2008), is used to model residual map patterns (e.g., high land prices near Tokyo).

The semiparametric model is fitted to the officially assessed residential land price data for every five years between 1985 and 2020 provided by NLNI ($N = 311,229$) using the R package mgcv (https://cran.r-project.org/web/packages/mgcv/index.html). The resulting (conditional) R-squared value is 0.744.

After estimation, the land price at each grid in year $t \in \{2025, 2030, \ldots, 2200\}$ is predicted for each population scenario by substituting the gridded population (and neighboring population) projected in each scenario into the estimated model. The fixed effects by city are given based on the projected urban extent. In other words, the fixed effect of the city u is assumed for the grids which are projected to be inside the city u in each year. The other covariates are assumed constant over years.

Figure 38 shows the total price of land in the country along with that in all cities during the 1970–1920 period in the baseline scenario. The total price of land will decrease by 24% (30%) between 2020 and 2120, while that of cities will decrease by 35% (44%) in the baseline (pessimistic) scenario. Thus, in the baseline (pessimistic) scenario, the urban area experiences greater land depreciation than the rural area. The flattening of cities results in a relatively greater depreciation of land prices in larger cities. Specifically, the total price of land in the three largest cities, Tokyo, Osaka and Nagoya, will decrease by 38% (48%) in the baseline (pessimistic) scenario.

[8] Available from the NLNI: https://nlftp.mlit.go.jp/ksj/.

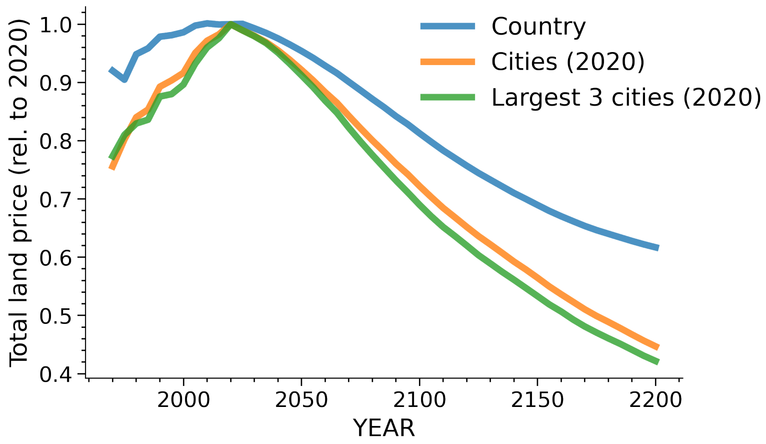

Figure 38. Projected total land price in the country and cities

Notes: The blue, orange, and green graphs show the evolution of the (nominal) total land price in the country, in the cities, and in the largest three cities, respectively, for the period 1970–2200. The values between 1970 and 2020 are realized values, while those in later years are projected values under the baseline projection of the country's population.

6 Alternative scenarios for distance frictions

So far, we have assumed that the rate of reduction in distance frictions over the past 50 years will continue into the future. However, it may be accelerated by advances in automated logistics systems and virtual communication technologies. To get to this point, we consider two alternative scenarios, one in which distance frictions decrease more substantially in the future than in the past 50 years, and the other in which the 2020 level of distance frictions persists in the future.

6.1 Faster reduction in distance frictions

First, we set the distance frictions to decrease faster than in the last 50 years, while assuming the baseline scenario for population decline. This can be achieved by assuming a faster decrease in the value of B_t in eq. (4), and hence a negatively larger value of a_1^B in eq. (3). Since the steeper city-size distribution (due to a negatively larger value of B_t) will reduce population size more for the smaller cities, some cities at the smallest end of the city-size distribution will disappear, resulting in a smaller number of cities. We set the rate of reduction in B_t so that the number of cities in 2120 is roughly the same as in the pessimistic scenario.

Specifically, we replace the PL model (4) with

$$\hat{P}^{Fast}_{u,t+1} = (1 - g_{t+1})\hat{P}_{u,t+1} + g_{t+1}\hat{P}^{Fast0}_{u,t+1} \tag{14}$$

where $\hat{P}_{u,t+1}$ is the estimated population size of city u in time $t+1$ using eq. (4), while

$\hat{P}^{Fast0}_{u,t+1}$ is obtained from an alternative power-law model that assumes a faster reduction in distance frictions by replacing a_1^B in eq. (3) estimated in the baseline scenario with $50 \times a_1^B$ and adjusting a_1^A so that $\hat{P}_{u,11} = \hat{P}^{Fast}_{u,11}$ (t=11 is the year 2020). The time-growing weight $g_{t+1} = \frac{t-11}{47-11}$ takes the value zero at $t = 11$ (2020) and one at $t = 47$ (2200). Thus, the reduction in distance frictions gradually accelerates over time starting in 2020.

The blue graph in Figure 39 shows the number of cities over time in the current scenario, while the orange graph is the baseline case. Compared to the baseline, the faster decline in transportation costs facilitates concentration toward the largest cities, as the theory suggests, and eliminates a number of the smallest cities. The number of cities will decrease by 219 between 2020 and 2120 in the current scenario, compared to 162 in the baseline.

Figure 40 shows the city-size distribution in 2020 (in blue), along with that in 2120 under the baseline scenario (in light blue) and that in 2120 under the current scenario (in orange). The figure shows that the largest cities are almost unaffected by the faster decline in distance frictions. This is because the population sizes of the disappearing small cities are very small compared to those of the largest cities. For example, Tokyo almost halves in both population size and maximum population density between 2020 and 2120 in both the current and baseline scenarios. Thus, the faster reduction of distance frictions essentially results in the elimination of a larger number of small cities, making the regional economy more dominated by large cities.

Recall that we assumed that the number of cities in the current scenario is similar to the number of cities in the pessimistic scenario in 2120. The main difference between the current scenario and the pessimistic scenario is that the population sizes of cities at the largest end of the city-size distribution become smaller in the latter scenario as a result of the country's population decline. For example, Tokyo's population size will decrease by 50% between 2020 and 2120 in the current scenario, while it will decrease by 65% in the pessimistic scenario.

6.2 Invariant distance frictions

For comparison, we consider a scenario that assumes time-invariant values of A_t and B_t so that the PL model assumes the power law coefficient as of 2020 persists into the future. In this case, the expected difference between $\log(P_{u,t+1})$ and $\log(P_{u,t})$ is given by taking the difference between the PL models (1) at time $t+1$ and t as follows:

$$E[\log(P_{u,t+1}) - \log(P_{u,t})] = \hat{B}(\log(R_{u,t+1} - 0.5) - \log(R_{u,t} - 0.5)) \tag{15}$$

where $\hat{B}$ is estimated by fitting eq. (1) on the data in 2020. The first and third terms in eq. (1) are canceled out because their expectations are time invariant. Given $P_{u,t}$, the expectation of $P_{u,t+1}$ yields:

$$\hat{P}^{Invariant}_{u,t+1} \equiv E[P_{u,t+1}] = P_{u,t} \exp[\hat{B}(\log(R_{u,t+1} - 0.5) - \log(R_{u,t} - 0.5))]. \tag{16}$$

The expected population changes only if the city rank changes between the time periods $t+1$ and t. We will use $\hat{P}^{Invariant}_{u,t+1}$ in the time-invariant scenario.

Compared to the baseline scenario, the smallest cities are more likely to survive because there is less of a force facilitating concentration toward larger cities under invariant distance frictions. The green graph in Figure 39 shows the number of cities over time in the current scenario. The number of cities decreases by 141 in the current scenario, while it is 162 in the baseline scenario between 2020 and 2120. The gray graph in Figure 40 shows the distribution of city sizes in 2120 in the current scenario. As in the case of the faster decline in distance frictions above, the future population sizes of the largest cities are roughly the same as in the baseline scenario, since the population sizes of the small cities that managed to survive but were eliminated in the baseline scenario are small compared to those of the largest cities.

Thus, in the absence of future advances in transportation and communication technologies, there will be more opportunities for small rural cities to survive.

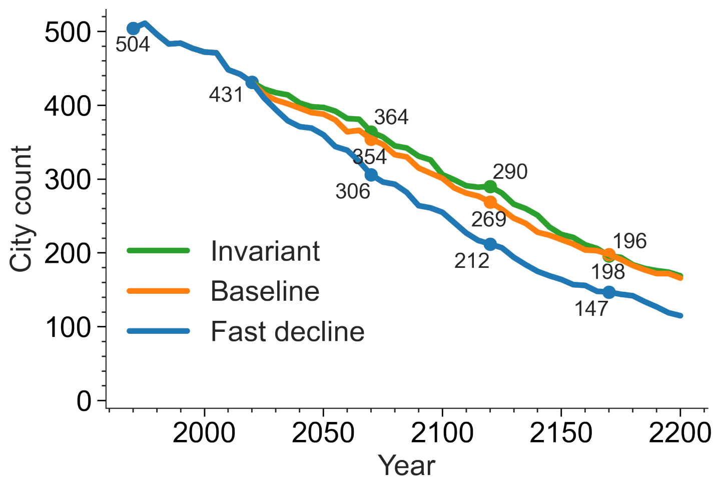

Figure 39. Predicted numbers of cities under alternative scenarios for the reduction in distance frictions

Notes: The predicted evolution of the number of cities under the three alternative scenarios regarding the reduction of distance frictions. The total population growth is given by the baseline scenario as in Section 5. The orange graph shows the baseline case as in Fig. 14. The blue graph shows the case of faster reduction of distance frictions, where the PL model (4) is replaced by (14), and the green graph shows the case where the power law coefficient B_t in eq. (1) is fixed at the value in 2020, i.e. the PL model (4) is replaced by (16).

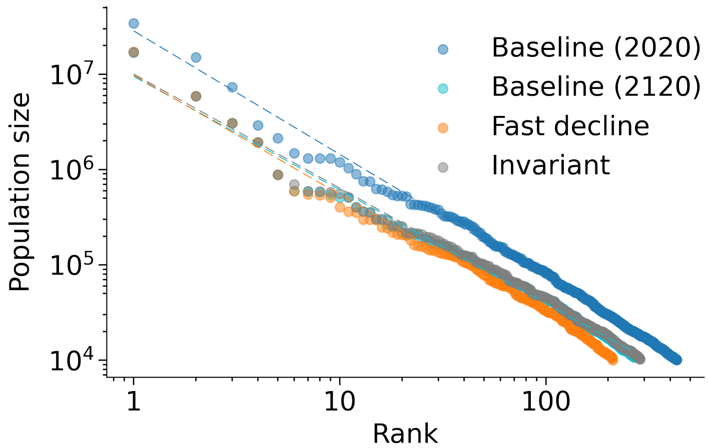

Figure 40. City-size distributions under alternative scenarios regarding the decline of distance frictions.

Notes: The blue and light blue scatter plots are the city-size distributions of the baseline case in 2020 and 2120, respectively, which are the blue and green plots, respectively, in Fig. 15A. The orange and grey plots are the city-size distributions in 2120 under the fast reduction of distance frictions and under the invariant distance frictions, respectively, with the baseline projection of the total population. Dashed lines are the fitted regression lines.

7 Concluding remarks

In this paper, we have developed a statistical model to forecast the future distribution of population across grid cells in a country. Specifically, our forecasting model ensembles a statistical model that accounts for the country-level regularity of a power law for city sizes and those that account for city- and grid-specific growth factors, where each city is treated as an endogenous population agglomeration whose spatial area changes over time.

Given the official projection of the country's population decline, together with the trend of decreasing distance frictions experienced in Japan over the past 50 years, we predicted the population distribution over the 1-km grids in Japan in the coming century.

Theoretical consistency – The estimated evolution of future geographic population distribution in Japan is consistent with the equilibrium and comparative static properties implied by economic agglomeration theory, in which both inter- and intra-agglomeration spaces are explicitly modeled (Akamatsu et al., 2023; Osawa and Akamatsu, 2020; Mori et al., 2023a).

Under the unprecedented population decline in Japan due to aging and decreasing distance frictions, we found that regional populations do not simply decline proportionally. The smaller cities tend to decline first, while the population of these depopulated cities is absorbed by the largest cities. However, large cities are also subject to crowding out due to tougher competition under decreasing distance frictions. As a result, there will be fewer larger cities that are mutually farther apart.[9]

Place-based policies

The results in Section 5.2 suggest that the largest cities that are farther apart tend to survive in the future. For example, in the west of Tokyo, the fourth largest city, Fukuoka, continues to show positive growth in population share, while the second and third largest, Osaka and Nagoya, will decline. This uneven growth of cities is consistent with the *country-level concentration* in models of endogenous economic agglomeration, where more globalized competition leads firms and households to concentrate in fewer and larger cities as distance frictions decline. Namely, Osaka and Nagoya will become too close to Tokyo for their size, entering Tokyo's agglomeration shadow, while the fourth largest city, Fukuoka, is far enough away to escape the shadow.

More generally, we are expected to see that the number of cities of a given size or larger will decrease, and the surviving cities will be further apart from each other, as we saw in the change in the geographic distribution of focal cities in Section 5.4. This has important implications for the appropriateness of place-based policies promoted across the country.

For a government-designated Life Zone to maintain basic infrastructure and functions for living in Japan, the minimum threshold population size is considered to be 100,000. The number of cities with at least 100,000 was already 83 in 2020. It is then predicted to decrease to 62 in 2070 and to 49 in 2120 in the baseline scenario. At present, however, as many as 675 municipalities are trying to revitalize themselves as cities by compacting their urban areas in accordance with the national "compact city policy."[10]

However, rather than fighting for population and reurbanization, it may be preferable for these communities to transform themselves into productive rural areas that take advantage of their rich agricultural and natural resources in Japan without advocating urbanism. Assuming that the population drops to 30–50 million in 100 years, Japan may be able to become self-sufficient in many agricultural products if proper farmland development is promoted now.

[9]This strong dependency between the population size and spacing of cities cannot be accounted for by the systems-of-cities models (e.g., Behrens et al., 2014; Duranton and Puga, 2014, 2023), perhaps the most popular framework today, as they lack the role inter-city space in determining the size and growth of cities.

[10]It has been reported at the first meeting of the Study Group for Improving the Effectiveness of the Location Appropriateness Plan by the MLIT on December 15, 2023 (https://www.mlit.go.jp/toshi/city_plan/content/001712725.pdf).

Housing demand and policies

Within each city, population distribution generally flattens in the future, which is consistent with the *city-level dispersion* exhibited by models of endogenous economic agglomeration, where congestion costs are more pronounced with less distance frictions within a city.

We found in Section 5.8 that between 2020 and 2120 in the baseline scenario, the average and maximum population densities are projected to decrease by 12% and 23%, respectively, on average for all cities, while these numbers are more substantial, 41% and 51%, respectively, in Tokyo. As a result, the total price of land in the urban area as of 2020 is expected to decrease by 35% between 2020 and 2120, while there will be a decrease of 39% in Tokyo during the same period.

Here we consider two implications of these projections. First, the demand for high-rise buildings in the central business districts of cities is expected to decline sharply in the future. Since houses and office buildings are durable goods, it is desirable for the government to proactively guide the shift to low-rise residential buildings. Second, the lower land prices in the future may allow households to consume more living space, which may ease the space constraints for households to have children. The expected substantial decline in land prices, especially in large cities such as Tokyo, may encourage higher fertility in these cities and mitigate the rate of population decline.

Soft landing of shrinking metropolises

Another important finding of this paper is that, with the exception of Tokyo and Fukuoka, the population of most major cities is expected to decline more than the population of the country. When a large city declines, the amount of housing and urban infrastructure does not immediately decrease because housing and infrastructure are durable. As a result, housing and office rents will drop. The lower rents cause a vicious cycle in which the residents of these cities are replaced by lower-income groups, thereby slowing the decline of the urban population while worsening public safety. This problem is common to many cities, such as Detroit, that once specialized in heavy manufacturing in the so-called rust belt of the United States (e.g., Glaeser and Gyourko, 2005). These declining major cities require careful urban planning beyond housing policies that anticipate future shrinkage and lower densities.

Future agenda

Based on the future projections of the geographic distribution of the population obtained in this paper, future projections can be attempted for a variety of important indicators. Below, we discuss two possible extensions of our model for future work.

Industrial Location

The population size of a city has been shown to be a strong predictor of the presence of a given industry in the city, with the set of industries present in a smaller city being roughly the subset of those present in a larger city (Mori et al., 2008; Hsu, 2012; Schiff, 2015; Mori et al., 2023a). Such coordination of the location behavior of industries has already been microfounded by the modern central place theory (e.g., Fujita et al., 1999; Tabuchi and Thisse, 2011; Hsu, 2012; Davis and Dingel, 2020; Mori et al., 2023a). Using this strong regularity, it is in principle possible to determine the future industrial composition of cities. From the industry's point of view, it is possible to predict the future set of feasible cities for operation in the shrinking economy.

Pollution and disaster risk management

The intensity of carbon dioxide emissions can be estimated from the population density of each location and the population size of the city to which the location belongs from future projections of the geographic distribution of the population. An earlier attempt in this direction can be found in Yamagata et al. (2017). Similarly, disaster risk at any point in time can be predicted from the geographic distribution of population, and, for example, those of earthquake and flood risk. As population decline eases space constraints for both commercial and residential locations, carbon dioxide emissions and disaster risk can be reduced through appropriate zoning. By incorporating zoning constraints into the forecasting model developed in this paper, it is possible to simulate optimal zoning and quantitatively evaluate its effects.

Appendix

A Urban agglomerations

Each *Urban Agglomeration* (*UA*) in a given time $t = \{1, \ldots, 36\}$ (corresponding to years, 1970, 1975, ..., 2200) is identified as the set of 1km grid cells that (i) have a population density of at least 1,000 per square kilometer, (ii) are geographically contiguous, and (iii) have a total population of at least 10,000 in time t.

The set of UAs is updated every $t = \{1, \ldots, 36\}$. We keep track of each UA over time by assigning it a unique identifier (ID) throughout the study period as follows:

1. IDs of UAs in time $t = 1$ are set to be their city size ranking in t. For those with the same population size, UAs are ranked according to their average population density in descending order.
2. A UA at time t and a UA at time $t+1$ are considered the same if they share the largest population as of time t in their areal intersection. (If there are multiple ties, the pair with the largest population density in their areal intersection takes the precedence.) In this case, their IDs at time $t+1$ are inherited from time t.
3. If UA i in time t has the largest population at time t in the areal intersection with UA j in time $t+1$, and UA j in time $t+1$ has the largest population in the areal intersection with a UA other than i in time t, then UA i is considered to be absorbed by UA j in time $t+1$.
4. If UA j in time $t+1$ has no intersection with any UA in time t, then UA j is considered to be either a newly formed UA or a UA split from an existing UA. For a newly formed UA or a split UA with no predecessor in older time $< t$, a new ID is assigned in the descending order of their population size in time $t+1$ (in the case of a tie, the one with the highest average population density is assigned an ID first).
5. If a UA is split from the existing UA at time $t+1$, but has a predecessor at time before t, the ID of the latest predecessor is restored. If there are multiple most recent predecessors, the one with the largest population in the areal intersection with the UA is chosen (again, in the case of a tie, the predecessor with the largest average population density is chosen). Thus, a UA i that was absorbed once by another UA j and later split from UA j will be renamed i again.

B Projection procedure

We project city populations in 2025–2200 by 5 year corresponding to the time index $t \in \{12, \ldots, 36\}$, by using the population data in 1970–2020 corresponding to $t \in \{1, \ldots, 11\}$. First, we perform the following pre-processing:

B.1 Parameter estimation

We first estimate the model parameters as follows.

1. Identify cities in $t \in \{1, \ldots, 11\}$ through the procedure explained in Section A.
2. For each city existing in $t = 11$, fit ARI1, ARI2, CS, and LL on the data in $t \in \{1, \ldots, 11\}$, and estmate their parameters.
3. Estimate the parameters of the PL model as follows:
   (a) By $t \in \{1, \ldots, 11\}$, fit the PL model (1) on the city population data to estimate the parameters $\hat{A}_t | t \in \{1, \ldots 11\}$ and $\hat{B}_t | t \in \{1, \ldots 11\}$.
   (b) Forecast $\hat{A}_t | t \in \{12, \ldots 36\}$ by fitting the LL model (2) on $\hat{A}_t | t \in \{1, \ldots 11\}$. Forecast $\hat{B}_t | t \in \{12, \ldots 36\}$ in the same manner.

B.2 City-level projection

1. **PL-model projection** – For each city u, project $\hat{P}^{PL}_{u,t+1}$ by substituting the parameters $\hat{A}_t, \hat{B}_t$, the rank $R_{u,t}$, and the previous population $\hat{P}_{u,t}$ into the PL model (4).
2. **Model ensemble** – For each city u, average the time-series model-based predictor $\hat{P}^{TS}_{u,t+1}$ given by (9) and the PL-based predictor $\hat{P}^{PL}_{u,t+1}$ given by (4) to obtain $P_{u,t+1}$ given by (10).
3. **Population rescaling** – For each t, rescale $\hat{P}_{u,t+1} | u \in \mathbf{U}$ to equate their sum to the total urban population that is exogenously given (Section 3).

For cities which are newly born, time-series models are not available because of the absence of past observations. For cities formed after 2025, zero weights ($W^M_u = 0$) are assumed for ARI1, ARI2, and LL in step 2, and only the PL model is used for the prediction of their future population size.

B.3 Grid-level projection

The grid populations $p_{i,t}$ in $t \in \{11,\ldots,35\}$ corresponding to $\{2025,\ldots,2195\}$ are projected to those in time $t+1$ in the procedure below. In particular, given the geographic population distribution $p_{i,t}$ over the grids $\mathbf{G}$ in time t, we compute an expected geographic distribution of the population over $\mathbf{G}$ in time $t+1$ (see steps 3–6 below), taking into account the growth factors at the city and country levels.

1. **Projection by each model** – By grid, project populations $\hat{p}^{m}_{i,t+1}|m \in \{ARI1, ARI2, CL, LL, SARI1, SARI2, SCL, SLL\}$ by using the parameters estimated a priori using the data up to 2020.

2. **Model ensemble** – By grid, substitute the projected populations into eq. (12) to obtain the expected population projection $\hat{p}_{i,t+1}$.

3. **City reidentification** – Identify cities using $\hat{p}_{i,t+1}|i \in \{1,\ldots,n\}$, according to the procedure explained in Section A. Denote the reidentified set of cities $\mathbf{U}'_{t+1}$. Then, update the city ranking $R_{u,t+1}$ for $u \in \mathbf{U}'_{t+1}$.

4. **City-level projection update** – Using the updated ranking $R_{u,t+1}$ of cities, perform the city-level projection (Step 1 in Section B.2) to evaluate the $\hat{P}_{u,t+1}$ of the updated city u.[11] Note that in general the reidentified set of cities, $\mathbf{U}'_{t+1}$, and the original one are not the same, i.e., $\mathbf{U}'_{t+1} \neq \mathbf{U}_{t+1}$. For cities $u \in \mathbf{U}'_{t+1} \backslash \mathbf{U}_{t+1}$, we do not have the observed time-series data. For these cities, we use only the PL model to obtain $\hat{P}_{u,t+1}$, i.e., we set $W^{PL}_{u} = 1$ and $W^{M}_{u} = 0\ \forall M \in \{ARL1, ARL2, CS, LL\}$.

5. **Rescaling** – For each city $u \in \mathbf{U}'_{t+1}$, rescale the population $\hat{p}_{i,t+1}$ in grid $i \in \mathbf{U}'_{u,t+1}$ in the city, to equate their sum with $\hat{P}_{u,t+1}$. In addition, rescale the projected grid populations outside cities $p_{j,t+1}$ for $j \notin \mathbf{U}'_{u,t+1}\ \forall u \in \mathbf{U}'_{t+1}$ to equate the total population of grids with the total population in Japan in $t+1$, which is exogenously given.

6. **Smoothing** – The projected population $\hat{p}_{i,t+1}$ is smoothed to avoid discontinuity at the city borders. The smoothing is done by taking the weighted average of the projected population $\hat{p}_{i,t+1}$ and the average of the population $\hat{Q}_{i,t+1} = \frac{1}{9}\Sigma_{i_{9NN}}\hat{p}_{t+1,i_{9NN}}$ in the 9NNs. The weight for $\hat{p}_{t+1,i}$ is given by $\Sigma_{m\in\{ARI1,ARI2,CS,LL\}}w^{m}_{i,t}$ which is the cumulative weight for the four pure time-series models while the weight for $\hat{Q}_{i,t+1}$ is given by $\Sigma_{m\in\{SARI1,SARI2,SCS,SLL\}}w^{m}_{i,t}$ which is the cumulative weight for the spatial time-series models.

[11] Here, the city-level projection is to find a stationary state of the city-size distribution, rather than the prediction of the next-period city sizes.

7. **Iterations** – If $\mathbf{U}'_{t+1} \neq \mathbf{U}_{t+1}$, we set $\mathbf{U}'_{t+1} \coloneqq \mathbf{U}_{t+1}$, and repeat steps 3–6 until the city set converges, i.e., $\mathbf{U}'_{t+1} = \mathbf{U}_{t+1}$.

C Predicted geographic population distributions

Figures 41–45 show the population distribution over the 1km grid cells around Tokyo in years, 2050, 2070, 2120, and 2170, in each scenario considered in the main text. Each panel in the figures is linked to a web map showing the geographic distribution of the population in the entire study area of Japan which can be scrolled and zoomed in. Figure 41 additionally contains the maps of the realized population distribution in 1970 and 2020 in Panels A and B, respectively.

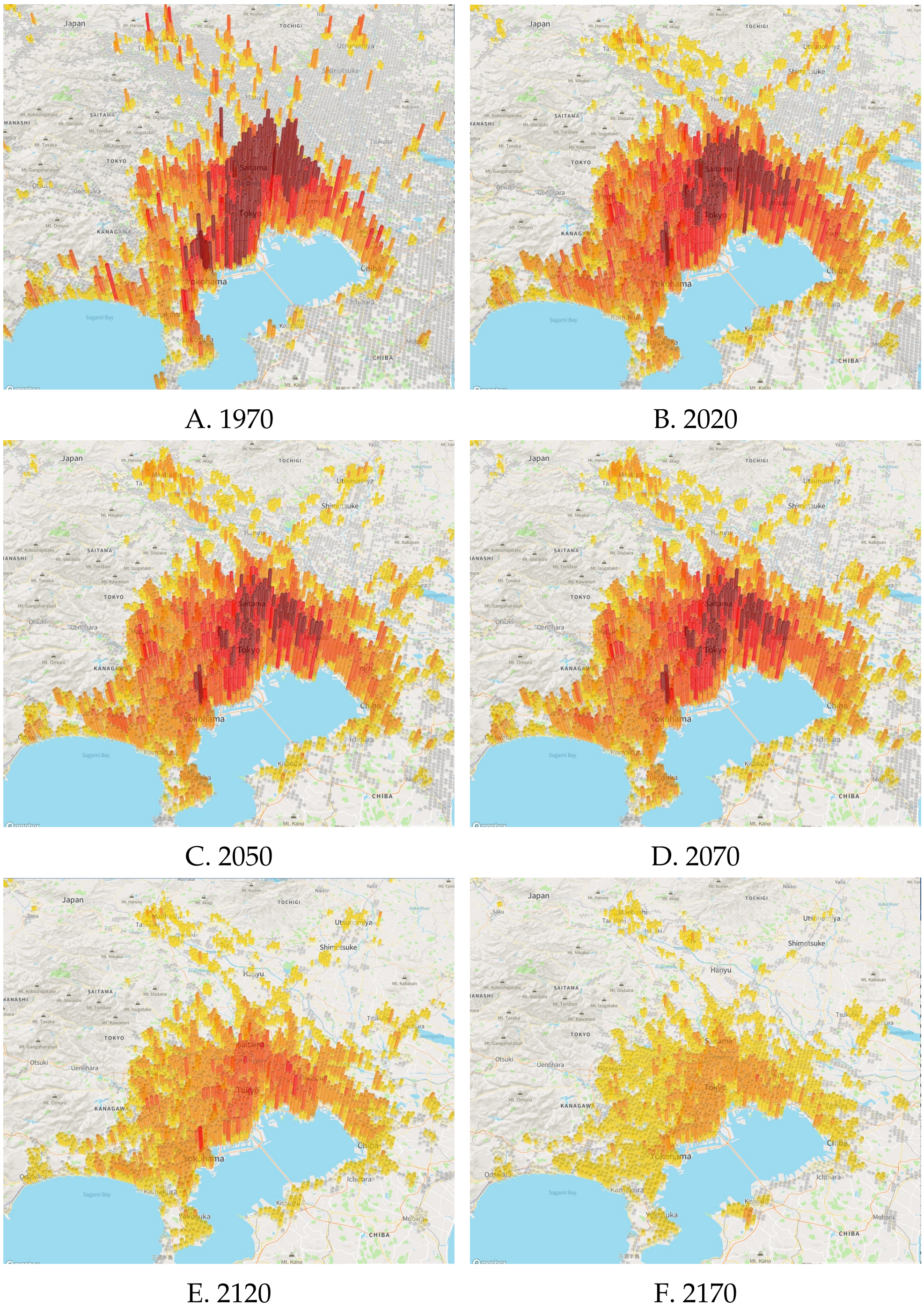

A. 1970 B. 2020

C. 2050 D. 2070

E. 2120 F. 2170

Figure 41. Geographic population distribution: 1970–2170 (Baseline)

Notes: (A–F) show the projected population distribution over 1km grid cells around Tokyo UA in 1970, 2020, 2050, 2070, 2120, and 2170, respectively, in the baseline scenario. Each panel is linked to a web map showing the geographic distribution of population in Japan, which can be scrolled and zoomed. Yellow and warmer colors indicate the grid cells with a population density of at least 1,000. The correspondence between the color of the bar and the population density in a grid cell is the same as shown in Fig. 34.

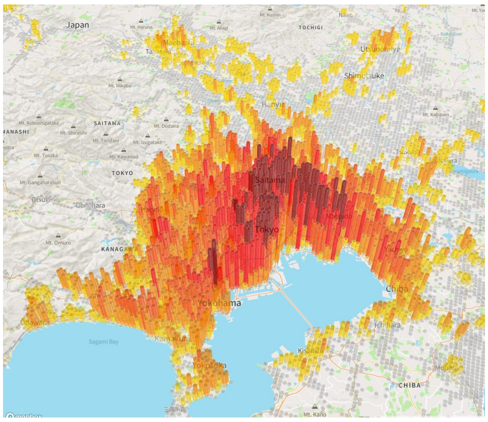

A. 2050

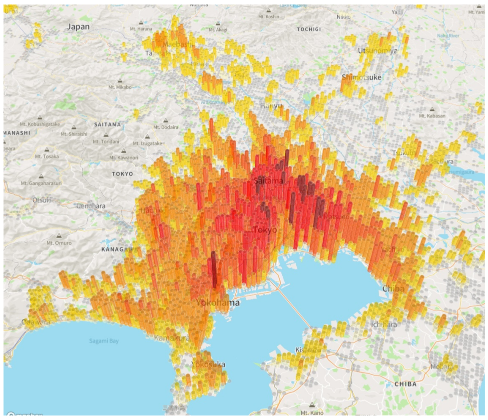

B. 2070

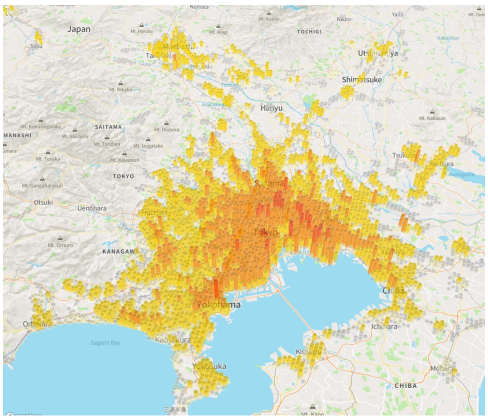

C. 2120

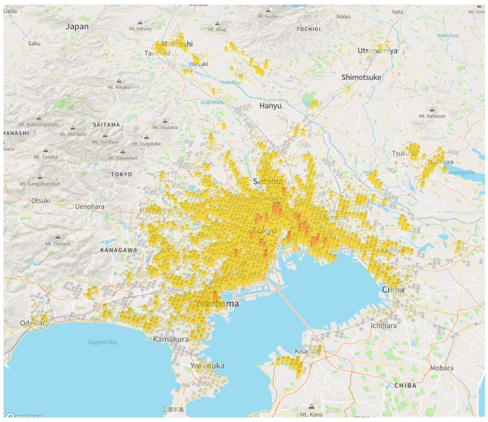

D. 2170

Figure 42. Geographic population distribution: 1970–2170 (Pessimistic)

Notes: (A–F) show the projected population distribution over 1km grid cells around Tokyo UA in 2050, 2070, 2120, and 2170, respectively, in the pessimistic scenario. Each panel is linked to a web map showing the geographic distribution of population in Japan, which can be scrolled and zoomed. Yellow and warmer colors indicate the grid cells with a population density of at least 1,000. The correspondence between the color of the bar and the population density in a grid cell is the same as shown in Fig. 34.

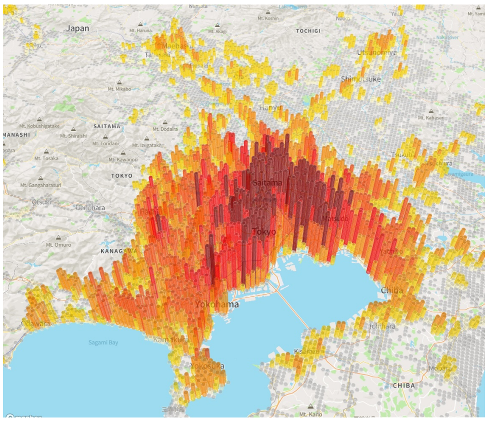

A. 2050

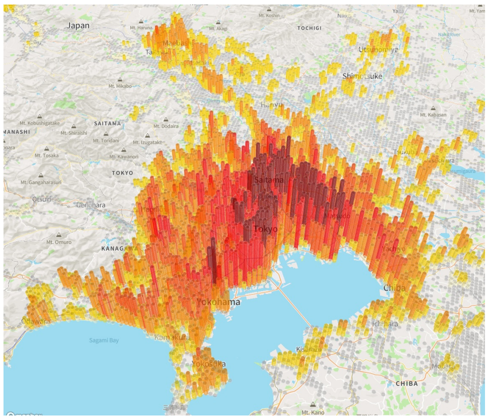

B. 2070

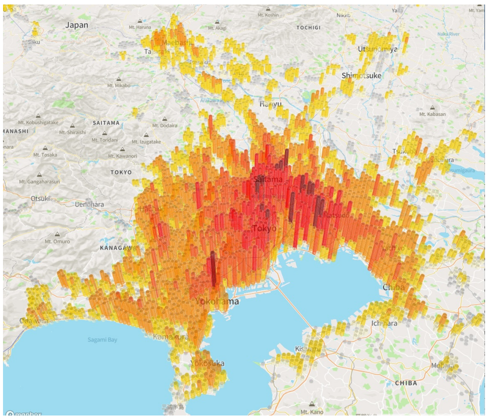

C. 2120

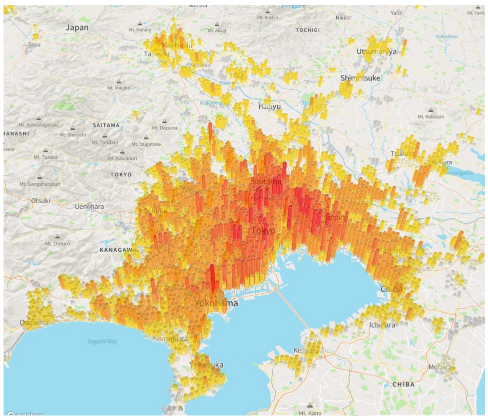

D. 2170

Figure 43. Geographic population distribution: 2050–2170 (Optimistic)

Notes: (A–F) show the projected population distribution over 1km grid cells around Tokyo UA in 2050, 2070, 2120, and 2170, respectively, in the optimistic scenario. Each panel is linked to a web map showing the geographic distribution of population in Japan, which can be scrolled and zoomed. Yellow and warmer colors indicate the grid cells with a population density of at least 1,000. The correspondence between the color of the bar and the population density in a grid cell is the same as shown in Fig. 34.

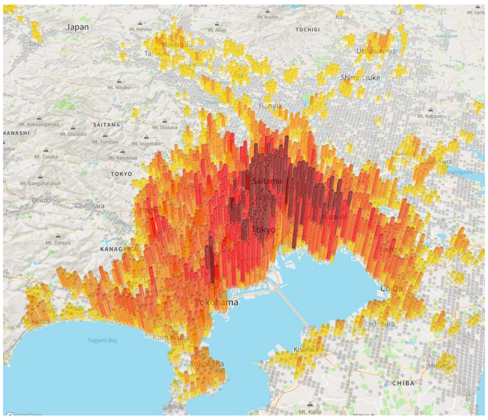

A. 2050

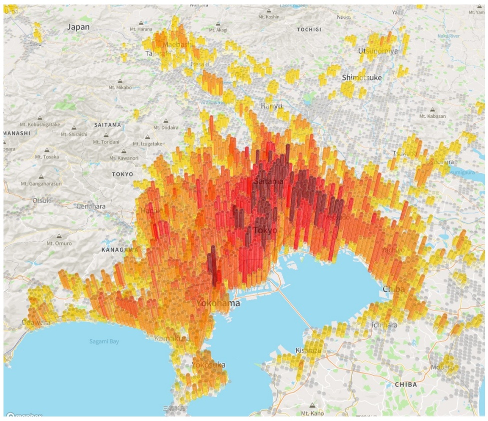

B. 2070

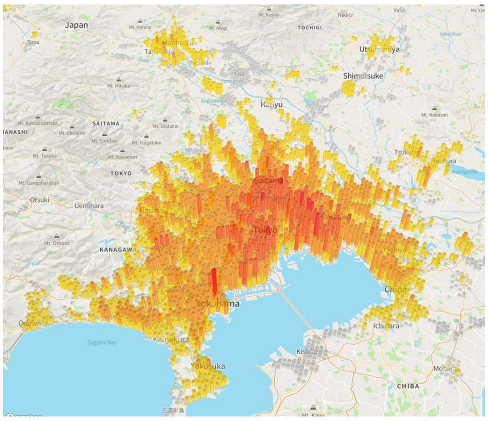

C. 2120

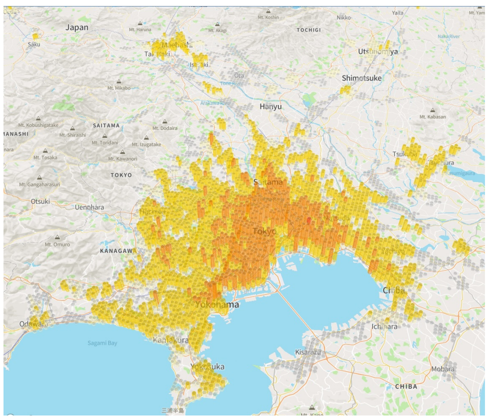

D. 2170

Figure 44. Geographic population distribution: 2050–2170 (Fast reduction in distance frictions)

Notes: (A–F) show the projected population distribution over 1km grid cells around Tokyo UA in 2050, 2070, 2120, and 2170, respectively, in the scenario with faster reduction of distance frictions. Each panel is linked to a web map showing the geographic distribution of population in Japan, which can be scrolled and zoomed. Yellow and warmer colors indicate the grid cells with a population density of at least 1,000. The correspondence between the color of the bar and the population density in a grid cell is the same as shown in Fig. 34.

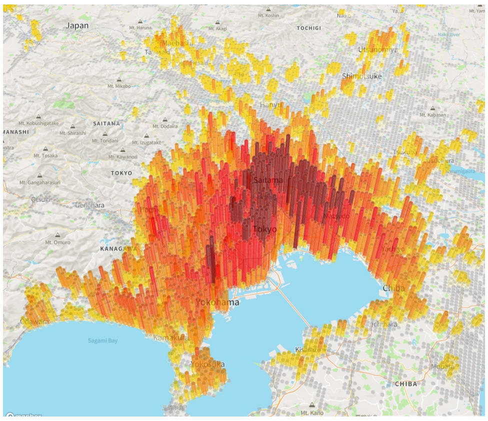

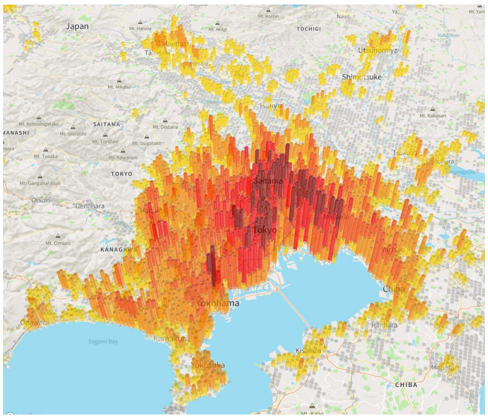

A. 2050 B. 2070

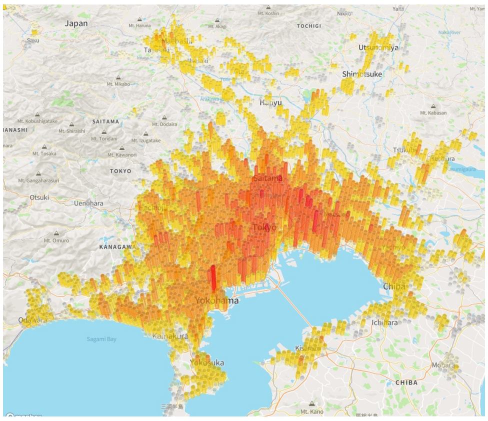

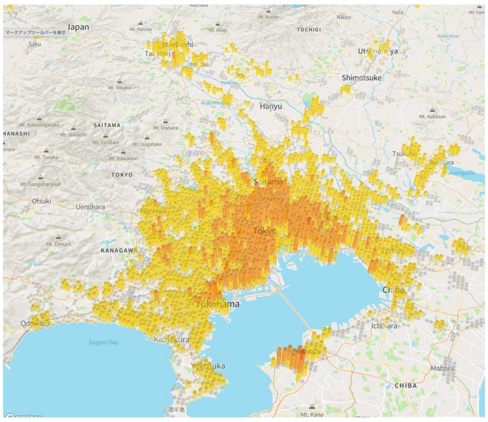

C. 2120 D. 2170

Figure 45. Geographic population distribution: 1970–2170 (Invariant distance frictions)

Notes: (A–F) show the projected population distribution over 1km grid cells around Tokyo UA in 2050, 2070, 2120, and 2170, respectively, in the scenario with invariant distance frictions. Each panel is linked to a web map showing the geographic distribution of population in Japan, which can be scrolled and zoomed. Yellow and warmer colors indicate the grid cells with a population density of at least 1,000. The correspondence between the color of the bar and the population density in a grid cell is the same as shown in Fig. 34.

References

Akamatsu, Takashi, Tomoya Mori, Minoru Osawa, and Yuki Takayama, "Endogenous agglomeration in a many-region world," 2023. arXvi:1912.05113.

Banerjee, Sudipto, Alan E Gelfand, Andrew O Finley, and Huiyan Sang, "Gaussian predictive process models for large spatial data sets," *Journal of the Royal Statistical Society Series B: Statistical Methodology*, 2008, *70* (4), 825–848.

Behrens, Kristian, Gilles Duranton, and Frédéric Robert-Nicoud, "Productive cities: Sorting, selection, and agglomeration," *Journal of Political Economy*, June 2014, *122* (3), 507–553.

Box, George EP, Gwilym M Jenkins, Gregory C Reinsel, and Greta M Ljung, *Time series analysis: forecasting and control*, John Wiley & Sons, 2015.

Bromiley, Paul, "Products and convolutions of Gaussian probability density functions," *Tina-Vision Memo*, 2003, *3* (4), 1.

Cohen, Samuel, Rendani Mbuvha, Tshilidzi Marwala, and Marc Deisenroth, "Healing products of Gaussian process experts," in "International Conference on Machine Learning" PMLR 2020, pp. 2068–2077.

Davis, Donald R. and Jonathan I. Dingel, "The Comparative Advantage of Cities," *Journal of International Economics*, 2020, *123*, 103291.

Duranton, Gilles and Diego Puga, *The growth of cities*, Vol. 2 of Handbook of Economic Growth, Amsterdam: North-Holland,

_ and _ , "Urban growth and its aggregate implications," *Econometrica*, November 2023, *91* (6), 2219–2259.

Durbin, James and Siem Jan Koopman, *Time series analysis by state space methods*, Vol. 38, OUP Oxford, 2012.

Fujita, Masahisa and Paul R. Krugman, "When is the economy monocentric?: von Thuünen and Chamberlin unified," *Regional Science and Urban Economics*, 1995, *25* (4), 505–528.

_ , Paul Krugman, and Tomoya Mori, "On the evolution of hierarchical urban systems," *European Economic Review*, 1999, *43*, 209–251.

Gabaix, Xavier and Rustam Ibragimov, "Rank- 1/2: a simple way to improve the OLS estimation of tail exponents," *Journal of Business & Economic Statistics*, 2011, *29* (1), 24–39.

_ **and Yannis M. Ioannides**, "The evolution of city size distributions," in J. Vernon Henderson and Jacques-François Thisse, eds., *Handbook of Regional and Urban Economics*, Vol. 4, Elsevier, 2004, pp. 2341–2378.

Glaeser, Edward L. and Joseph Gyourko, "Urban decline and durable housing," *Journal of Political Economy*, 2005, *113* (2), 345–375.

Graves, Alex, "Generating sequences with recurrent neural networks," *arXiv preprint arXiv:1308.0850*, 2013.

Hsu, Wen-Tai, "Central place theory and city size distribution," *Economic Journal*, 2012, *122*, 903–932.

Ministry of Health, Labour and Welfare of Japan, "Vital Statistics," 2022.

Ministry of Internal Affairs and Communications of Japan, "The Grid Square Statistics, The Population Census of Japan," 1970, 1975, 1980, 1985, 1990, 1995, 2000, 2005, 2010, 2015, 2020.

Ministry of Land, Infrastructure, Transport, and Tourism of Japan, "Land Market Value Publication," 1985–2020.

Mori, Tomoya, Koji Nishikimi, and Tony E. Smith, "The number-average size rule: A new empirical relationship between industrial location and city size," *Journal of Regional Science*, 2008, *48* (1), 165–211.

_ **, Takashi Akamatsu, Yuki Takayama, and Minoru Osawa**, "Origin of power laws and their spatial fractal structure for city-size distributions," 2023. arXiv:2207.05346.

_ **, Tony E. Smith, and Wen-Tai Hsu**, "Common power laws for cities and spatial fractal structures," *Proceedings of the National Academy of Sciences of the United States of America*, March 2020, *117* (12), 6469–6475.

_ **, Yosuke Kogure, Tatsuya Sugimoto, and Yuki Takayama**, "Structural model analysis of endogenous agglomeration: Application to Japanese cities," 2023. In progress. Kyoto University.

National Institute for Environmental Studies, Japan, "Shared socio-economic pathways – Municipality population scenarios, 2nd ed.," 2021.

National Institute of Population and Social Security Research, "Population Projections for Japan: 2021 to 2070 (With long-range Population Projections: 2071 to 2120)," 2023.

_ , "Regional Population Statistics of Japan," Technical Report 2023.

Osawa, Minoru and Takashi Akamatsu, "Equilibrium refinement for a model of non-monocentric internal structures of cities: A potential game approach," *Journal of Economic Theory*, 2020, *187*, 105025.

Polikar, Robi, "Ensemble learning," *Ensemble machine learning: Methods and applications*, 2012, pp. 1–34.

Schiff, Nathan, "Cities and product variety: Evidence from restaurants," *Journal of Economic Geography*, 2015, *15* (6), 1085–1123.

Smith, Stanley K, Jeff Tayman, and David A Swanson, "State and local population projections: Methodology and analysis," 2005.

Tabuchi, Takatoshi and Jacques-François Thisse, "A new economic geography model of central places," *Journal of Urban Economics*, March 2011, *69* (2), 240–252.

United Nations, "The 2018 Revision of World Urbanization Prospects," 2018.

_ , "World Population Prospects," 2022.

Wood, Simon N, *Generalized additive models: an introduction with R*, CRC press, 2017.

Yamagata, Yoshiki, Daisuke Murakami, and Takahiro Yoshida, "Urban carbon mapping with spatial BigData," *Energy Procedia*, December 2017, *142*, 2461–2466.